Duality violation from a grating

Daniel Mirell

Department of Chemistry, University of California,

Irvine, CA 92697, Electronic address: dmirell@uci.edu

Stuart Mirell

Department of Radiological Sciences,

University of California, Los Angeles,

CA 90024, Electronic address: smirell@ucla.edu

(Dated: July 6, 2011)

Abstract

Diffraction orders in the continuous wave regime generated by a Ronchi transmission grating in a standard threshold configuration are shown theoretically to violate quantum duality for a locally real representation. The phenomenon superficially resembles Rayleigh anomalies but is notably distinguished from those anomalies by a prediction of probability non-conservation. This prediction is experimentally tested with a 633 nm laser beam at normal incidence on gratings giving that threshold condition for the $\pm 3^{rd}$ order pair. Transient intersection of the 0^{th} order with an independent 633 nm laser beam demonstrates a duality-violating probability non-conservation in good agreement with the theoretical prediction.

I. INTRODUCTION

The compact mathematical formalism of quantum mechanics developed in the late 1920's continues as an extraordinarily successful representation of physical phenomena. The very compactness itself is widely perceived as evidence of the validity, beauty, and completeness of that formalism. This perception has persisted despite the evolving understanding over the years that strict adherence to the formalism imposes fundamental violations of classical physical reality. The resolution of these violations, given the constraints of that strict adherence, was understood by Bohr and others to necessarily impose a non-real and non-local representation of the physical world. This representation is often referred to as the probabilistic interpretation of quantum mechanics (PIQM) and consists of those postulates thought to rationally express the physical implications of the underlying compact quantum formalism.

The predictive validity of the quantum formalism is widely acknowledged. Nevertheless, the PIQM departures from local realism are not universally accepted. Lepore and Selleri [1] contend that "The development of local realism since the 1935 Einstein, Podolsky, and Rosen's paper [2] is by far the most profound criticism of quantum mechanics..." in reference to the probabilistic interpretation. Popper raises compelling philosophical arguments in questioning the validity of PIQM.[3]

The notable non-local properties of PIQM are manifestations of entanglement and wave-particle duality. Any viable local alternative to PIQM must minimally demonstrate an alternative self-consistent basis for both of these phenomena. In this regard, one of the present authors proposed a locally real representation of quantum mechanics that gives agreement with performed experiments for correlated photons and particles [4] and is not restricted by Bell's theorem.[5] The other phenomenon, wave-particle duality, is examined by the authors in ref. [6]. In this report we again examine wave-particle duality and propose a locally real representation of quantum mechanics, identified here as LRQM, that retains the accepted underlying quantum formalism with minimal modification.

As a preliminary matter, we first consider some elementary aspects of photon phenomena from the particular perspective of LRQM as distinguished from PIQM. In the discrete regime, a single photon is a physically real wave packet structure on which a real energy quantum resides. The LRQM wave function Φ characterizes the wave amplitude of this structure but

is not itself a physical representation of any resident energy quantum. The separability of these entities is identified with de Broglie's initial representations of quantum phenomena [7] and is intrinsic to many locally real representations.

Born interpreted the squared modulus of the wave function evaluated at particular coordinates as a measure of relative probability of finding a particle on a wave packet.[8] This initial restricted version of "Born's rule", applied here to electromagnetic radiation for LRQM, is critical in its treatment of the squared modulus $|\Phi|^2$ as a relative and not an absolute probability flux density. Saxon reminds us of the fundamental utility of the unnormalized $|\Phi|^2$ as the sufficient determining factor of relative positional probability.[9] The subsequent, commonly accepted interpretation of Born's rule incorporates normalization of the wave function giving unit absolute probability for the squared modulus integrated over the entire wave packet. Normalization is a seemingly natural and rational modification of the restricted version and was fully consistent with the then developing formulation of PIQM. This modification provides PIQM with a linkage of particle-like and wave-like properties that compactly expresses both in a wave function Φ_{PI} but necessitates the characteristic interpretations of duality and entanglement for particular phenomena.

Certainly, for an ordinary photon the resident particle-like energy quantum has unit absolute probability of existing somewhere on the wave packet and normalization of the LRQM wave function Φ in this case serves as a mathematical convenience in equating a unit-valued expression of energy conservation and a unit-valued probability represented by the integrated square modulus $|\Phi|^2$. Nevertheless, in LRQM an initial normalization of Φ must not be arbitrarily re-applied to an evolving wave function since processes such as interference occurring during that evolution may create or annihilate wave amplitude. Effectively, LRQM separates a purely wave-like Φ from a PIQM Φ_{PI} and provides that Φ with the degree of freedom to scale independent of resident quanta. We continue to use the term "probability" here in LRQM bearing in mind that its usage is potentially misleading since that term suggests equivalence to a mathematical absolute probability, an equivalence manifested in PIQM as duality.

Classically, the probability flux density $|\Phi|^2$ is recognized as a wave intensity. For a discrete photon incident on an idealized beam splitter, the wave intensity fractionally divides onto the output channels in accordance with the transmission and reflection coefficients of the beam splitter. In the present example, we choose for convenience a 50:50 beam splitter

for which the output packets are similar to the incident packet but with half the intensity giving each a relative probability of $P = 0.5$ when the incident packet is assigned $P = 1$. Then, when the energy quantum on that incident packet reaches the beam splitter, the quantum randomly transfers onto either of the emerging outgoing $P = 0.5$ packets with equal probability. In the discrete regime this implies that for each incident photon, one of the outputs is an "empty" wave that is totally "depleted" in energy quanta relative to its wave packet probability $P = 0.5$. Conversely, the other output is "enriched" in energy quanta relative to probability in the regard that the single energy quantum resides on a wave packet that is now $P = 0.5$ instead of $P = 1$. The prediction of empty waves in the discrete regime has been the subject of many investigations seeking to differentially test local realism and PIQM as in a series of papers by Croca et al. [10] as well as in numerous others such as refs. [11]. These investigations, frequently using a beam splitter to generate an empty wave, are necessarily restricted to the very weak wave intensities associated with discrete photon beams.

As we move from the discrete photon regime to a multiple photon beam in the continuous wave (cw) regime, the relevant total wave function is conventionally constructed from a summation over amplitudes of the constituent wave packets. (Our particular interest here is mono-energetic coherent beams.) The wave function, which we continue to identify as Φ, is used to express the beam's intensity $|\Phi|^2$, again a probability flux density. Integration of $|\Phi|^2$ over some selected beam segment gives an inclusive probability P. The corresponding inclusive quanta in that segment have a total energy E. We can set $P = E = 1$ in arbitrary units for the beam segment.

When this beam is incident on a 50:50 beam splitter, we again have $P = 0.5$ on each of the output channels. However, random statistical distribution of the inclusive quanta onto the output channels yields E vanishingly close to 0.5 on both channels as the inclusive number of quanta becomes large. An immediate consequence of the cw regime for the beam splitter is that testability for empty waves is no longer feasible. Then, although local realism does not expressly prohibit empty waves in the cw regime, the inherent statistical distribution process is intuitively expected to restrict all mechanisms for generating empty waves to the discrete regime where conclusive experimental verification is marginalized.

A mechanism that alters the proportionality of probability and energy on a photon beam in the cw regime is seemingly as improbable as Maxwell's hypothesized mechanism for

selectively sorting particles based upon their respective kinetic energies.[12]

In Section III. we present the theoretical basis for a mechanism that, from the perspective of LRQM, is predicted to selectively alter the proportionality of probability and energy. In Section IV. we report on the experimental realization of this phenomenon.

II. BACKGROUND

The theoretical basis developed here for the LRQM wave-like component is substantially classical. This basis does not obviate the underlying quantum mechanical formalism such as the wave function associated with quantization of the electromagnetic field, but it does modify the scaling of a separable, purely wave-like component Φ. As a consequence, the PIQM duality proportionality of wave probability (based on that Φ) and particle-like energy quantum is potentially violated. A mechanism for this duality violation, trivially but transiently realized in the discrete regime for LRQM, is however not immediately obvious in the cw regime. Before beginning the examination of mechanisms that achieve this "duality modulation" in the cw regime, we return to the example of a beam splitter once again in order to develop some basic operational definitions and principles relevant to LRQM.

When a photon is incident on a beam splitter, the transfer process of the energy quantum to one of the relative probability wave packets on the output channels is itself of fundamental significance to LRQM. For illustrative purposes we again choose a 50:50 beam splitter. The quantum on an incident $P = 1$ wave packet enters a zone at the face of the beam splitter where the quantum randomly transfers onto one of the two emergent $P = 0.5$ output wave packets. Unlike their treatment in PIQM, those output wave packets remain as real entities at that probability value on both output channels and one packet does not undergo a collapse when a measurement is made on the other packet.

From the perspective of LRQM, the transfer at the beam splitter must be treated purely as that of the energy quantum. Wave packet probability distribution is a non-quantized deterministic process at a device such as the beam splitter. The energy quantum arriving at the beam splitter surface randomly transfers onto one of the two emergent outputs causally mediated by their relative probability distribution consistent with Born's rule.[8] The wave structures of the two output packets are otherwise unaltered by the random presence or absence of the quantum on a particular output packet. (Conversely, we will subsequently

consider full photon transfers in other contexts that are consistent with both PIQM and LRQM, i.e. duality is not violated. Such transfers may involve scattering conditions that alter the trajectories of incident wave packets which are then accompanied by the proportionate energy quanta that had resided on the incident packets.)

In the interests of formalizing the proportionality between wave packet probability and energy quantum, we assign a value to their proportionality. Each photon on a discrete beam is represented by an "occupation" value $\Omega = E/P$ defined as the ratio of the energy quantum and the total probability of its wave packet.[6] As a baseline reference, we consider "ordinary" photons that might be generated by common atomic emission processes. We assign $E = 1$ to the energy quantum present on a wave packet of probability $P = 1$ giving $\Omega = 1/1 = 1$ for these ordinary photons in arbitrary dimensionless units.

If a discrete beam composed of such ordinary photons is incident on the 50:50 beam splitter, the output packets have $\Omega = 0/0.5 = 0$ and $\Omega = 1/0.5 = 2$. Any $\Omega < 1$ signifies that the outgoing wave packet is reduced in energy relative to its associated wave packet probability and is referred to as "depleted". In the extreme case of $\Omega = 0$, the wave packet is totally depleted and is appropriately referred to as an empty wave.[11] For $\Omega > 1$, the wave packet is said to be "enriched". In the present case of $\Omega = 2$, the single quantum resides on a $P = 0.5$ wave packet compared to the $P = 1$ wave packet of the incident photon.

In principle, interference of either outgoing wave packet $P = 0.5$ with an independent photon beam would result in the same visibility, unaffected by the presence or absence of the quantum on that outgoing wave packet. Fundamentally, a measurement such as interference visibility assesses a beam's wave-like property whereas a direct detector measurement assesses a beam's particle-like (energy quantum) property.

As a matter of practical consideration, measurements of the wave-like property in the discrete regime, as provided for example by beam splitter outputs, are experimentally problematic. [10] Accordingly, we are motivated to seek a duality violation in the cw regime where experimental verification is significantly enhanced.

In the cw regime, the irradiance I is used to describe the particle-like component of the photon beam where, conventionally, the formal units are those of an energy flux density. In contrast, the corresponding wave-like component is identified as the intensity $W = |\Phi|^2$ which, in the LRQM context, is exclusive of the energy content of the wave. In analogy to our use of arbitrary units for the discrete beam, we are free to set unit values for I and W

on an ordinary incident cw beam. Any value specification of flux densities such as I and W implicitly refers to a sample point on the beam and typically that sample point gives the maxima of those values e.g. at the beam centroid for a Gaussian cross-section.

With a specified I and W on an incident beam we have $\Omega = I/W$. Equilibration of energy quanta ensures that the Ω proportionality is maintained throughout the beam. Then

$$\begin{aligned} \Omega &= \frac{I}{W} \\ &= \frac{\int I(\mathbf{r},t)dadt}{\int W(\mathbf{r},t)dadt} \\ &= \frac{E}{P} \end{aligned} \tag{1}$$

where the areal integration is over the beam's cross-section and the integrands are the respective coordinate-dependent values of I and W. An inclusive energy E and probability P on a selected beam segment may be selected by a choice of temporal integration limits spanning some selected Δt. For that Δt, we are free to assign arbitrary units to these quantities on the incident beam that give $E = P = 1$ whereby $\Omega = 1$. Clearly, from the perspective of LRQM, $\Omega = 1$ is maintained on the outputs where, for a 50:50 beam splitter, $P = 0.5$ and, because of random statistical equilibration, $E = 0.5$.

As a result of the common equivalence of the I/W and E/P ratios on any given beam in the cw regime, we will have frequent occasion to consider either the I, W (maximum flux density) quantities or the E, P (integrated) quantities as a matter of illustrative convenience. Within the context of the present analysis, when E, P is the more convenient pair, the energy flux (power) $\Delta E/\Delta t$ and the probability flux $\Delta P/\Delta t$ would be equally convenient. However, we choose E, P in the interests of continuity with our earlier discussion of discrete photons.

As a reference baseline, an incident beam consisting of photons generated from conventional sources is identified as ordinary with $\Omega = 1$ by appropriate assignment of the arbitrary energy and probability units. Then the identifications of a cw beam as depleted or enriched are equivalently expressed by a respective $\Omega < 1$ or $\Omega > 1$.

We consider one last example involving the beam splitter, again 50:50, in which both input channels have mutually coherent similar incident cw beams with intensities

$$W_{ih} = W_{iv} = 0.5 \tag{2}$$

directed at the same point on the beam splitter and aligned so as to generate spatially

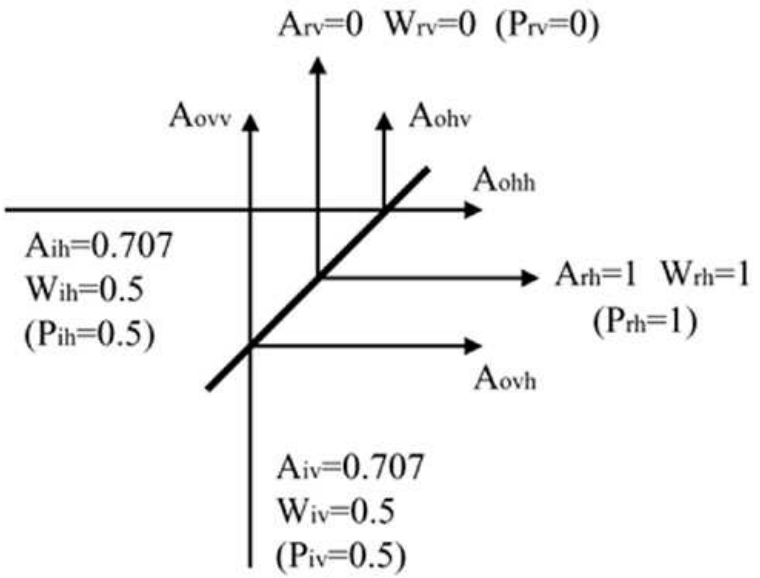

FIG. 1: Amplitude moduli associated with two identical mutually coherent beams coincident on a beam splitter depicted with lateral displacement for illustrative clarity. Outputs, that form resultants, continue propagating as real entities. For destructive phasing of A_{ovv} and A_{ohv}, the two incident beams are fully expressed by the resultant A_{rh} as an intensity output W_{rh}. Arbitrary numerical values are assigned for comparative purposes.

coincident outputs as identified in Fig. 1. In terms of the respective probabilities,

$$P_{ih} = P_{iv} = 0.5. \tag{3}$$

In this current example, we continue the convention of designating beam quantities as "incident" prior to interaction with a mechanism such as the beam splitter and "output" for the prompt post-interaction manifestations of those quantities. These post-interaction output quantities then generate physically distinguishable quantities by interference that are designated as "resultant". Clearly this distinction of output and resultant designations was superfluous for the previous example of a single beam incident on a beam splitter. Nevertheless, the utility of these designation distinctions will be evident when we consider duality modulating mechanisms.

In the present case, the two incident beams intersect at a common point on a beam splitter. In Fig. 1, the beams are laterally displaced from that common point in order

to clearly depict the various output and resultant components emanating from that point. The amplitude moduli of the two reflected and the two transmitted output beams all have identical values

$$A_{ohv} = A_{ovh} = A_{ohh} = A_{ovv} = 0.5 \tag{4}$$

with corresponding common intensity values

$$W_{ohv} = W_{ovh} = W_{ohh} = W_{ovv} = 0.25 \tag{5}$$

or, equivalently in terms of respective probabilities,

$$P_{ohv} = P_{ovh} = P_{ohh} = P_{ovv} = 0.25. \tag{6}$$

Then for total probabilities in the transition from incidence to output,

$$P_i = P_o = 1, \tag{7}$$

and probability is conserved in this incident→output transition.

Interference between the output beam amplitudes generates a pair of resultant beams with moduli dependent upon relative incident beam phasing. For our purposes here, we choose a particular phasing that gives amplitude moduli

$$A_{rh} = 1 \tag{8}$$

and

$$A_{rv} = 0 \tag{9}$$

with wave intensities

$$W_{rh} = 1 \tag{10}$$

and

$$W_{rv} = 0. \tag{11}$$

The output pair A_{ohh} and A_{ovh} is fully contiguous to its associated resultant A_{rh}, sharing a common origin at the beam splitter surface. The same applies to A_{ovv}, A_{ohv} and A_{rv}. In both cases, the members of either output pair are not separately experimentally measurable because interference of those members at their common origin promptly yields the experimentally measurable resultant wave. Nevertheless, these considerations do not alter

the continued reality of the output wave structures as they propagate contiguous to and are physically expressed by their respective resultant waves.

Integration yields the associated probabilities

$$P_{rh} = \int W_{rh}(\mathbf{r}, t) dadt = 1 \tag{12}$$

and

$$P_{rv} = \int W_{rv}(\mathbf{r}, t) dadt = 0 \tag{13}$$

where again, by appropriate choice of integration limits in arbitrary units, each has the same numerical value as that of the corresponding (maximum) wave intensity. With the total resultant probability

$$P_r = P_{rh} + P_{rv} = P_o = P_i = 1, \tag{14}$$

we have conservation of probability in the output→resultant transition as well as in the incident→output transition.

For our particular choice of relative phase, P_{rv} is identically zero and $P_{rh} = 1$. (That choice could also have been generalized as any relative phase but in anticipation of a relevant analogy in the next section, we choose a phase that gives a null value for one of the resultants.) For P_{rv}, the constituent output waves continue to propagate as real but π out-of-phase entities with a null sum. Similarly, the constituent in-phase output waves generate a resultant $P_{rh} = 1$ that exceeds the sum of those output probabilities,

$$P_{ohh} + P_{ovh} = 0.5. \tag{15}$$

These observations are very elementary and would have been superfluous for the absolute mathematical probabilities of PIQM. However, in the context of the real wave structures of LRQM, there is a significant process that should be emphasized here. Interference, which nullifies the resultant of the two output probabilities on one channel, fortuitously "amplifies" the output sum probability on the other channel to precisely compensate for that nullification and conserve probability in the output→resultant transition. The criticality of interference in conserving probability on these real wave structures suggests that a disruption of this precise compensation by interference may provide a mechanism for duality modulation.

Then with Ω's computed from either the I, W or the E, P pairs,

$$\Omega_{rh} = \Omega_{rv} = \Omega_r = 1 \tag{16}$$

respectively for the horizontal, vertical, and total resultant beam occupation values. These LRQM values are fully consistent with PIQM duality.

The various beam splitter phenomena treated here from the perspective of LRQM are, nevertheless, almost universally represented in the literature by a formalism consistent with PIQM. However, in the next section we analogously apply LRQM to particular grating systems and demonstrate the basis for a duality-violating mechanism that is not representable by PIQM.

III. THEORETICAL BASIS FOR DUALITY VIOLATION

A. Gratings with dense sampling

The general mechanism we consider here for modulating the ratio Ω of beam energy and probability is a conventional transmissive "picket-fence" grating consisting of a regular linear array of parallel opaque bands with a periodicity p forming intervening slits of width w. Typically for optical gratings of this type, the opaque bands are thin metallic depositions on one side of a transmissive substrate. In our analysis, we treat that side as the exit face of the transmission grating with an incident beam normal to the opposite face of the substrate.

As we proceed, we must take care to adequately quantify the real entities of energy and probability as incidence→output and output→resultant transitions occur. Ordinary incident beams generated by conventional sources may be assigned

$$P_i = E_i \tag{17}$$

in arbitrary units which gives an incident beam occupation value

$$\Omega_i = 1 \tag{18}$$

as a calculation convenience. The quantification at each transition requires either a verification that Ω is maintained or an individual assessment of energy and of probability in that transition.

For any individual slit, the output energy quanta and the output probability necessarily remain in constant proportionality relative to that of the incident beam since that single slit equally samples both quantities from the incident beam. Indeed, a deviation from this

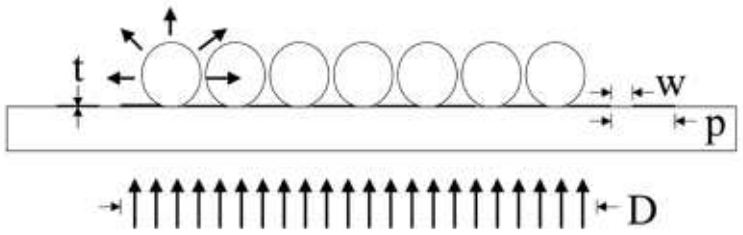

FIG. 2: Emergent output diffractive envelopes from N irradiated individual slits fully determine collective output probability (and energy) prior to the formation of resultant orders by interference as those envelopes intersect.

proportionality would constitute a violation of PIQM duality for a mechanism consisting of a single slit. Accordingly, from the perspective of LRQM as well as PIQM, an incident $\Omega_i = 1$ is maintained on the output of any single slit as well as collectively over all slit outputs, i.e. $\Omega_o = 1$. See Fig. 2.

Moreover, with an incident beam of some particular Gaussian diameter D, the (transmitted) output probability and output energy quanta are both invariant as w and p are proportionately varied since

$$w/p \equiv \sigma \tag{19}$$

presents a constant fractional cross section for transferring probability and energy quanta from incidence to output, i.e. the grating's transmission factor. Essentially, proportionate increases in w and p results in increases for individual slit outputs of both probability and energy quanta but, concurrently, the number of incident-irradiated slits yielding those outputs is proportionately decreased. Then, beginning with an ordinary incident beam, equal sampling gives the output quantities

$$P_{o;\sigma} = E_{o;\sigma} = 1, \tag{20}$$

where both are specific to some particular value of $\sigma = w/p$ but independent of w and, as a matter of convenience, in arbitrary units we assign unit value to both in Eq. (20). The output occupation value Ω_o is constructed from the ratio of $P_{o;\sigma}$ and $E_{o;\sigma}$ but, because of equal sampling for those quantities for any σ, their ratios

$$\Omega_o = \Omega_i = 1 \tag{21}$$

are independent of σ.

The transition to the resultant diffraction orders requires that we examine quantities such as wave amplitude and intensity for the emergent output diffraction envelopes. In this regard it is most expedient to begin with the classic phasor construction for the output wave intensity from a single slit W_{os} from Kirchhoff diffraction theory in the Fraunhofer approximation

$$W_{os}(\alpha) = W_{os}(0)\frac{\sin^2\alpha}{\alpha^2} = W_{os}(0)sinc^2\ \alpha \tag{22}$$

where

$$\alpha = \frac{\pi w}{\lambda}\sin\theta \tag{23}$$

for a wavelength λ. Eq. (22) above must be used with care as we proceed since the intensity $W_{os}(\alpha)$ is expressed in "α-space" rather than over the physical θ angular space azimuthal to the slit. Moreover, this phasor construction relates entirely to the slit output intensity distribution, giving $W_{os}(\alpha)$ relative to a centroid value $W_{os}(0)$. Effectively then, the Eq. (22) intensity is unscaled with respect to the incident beam intensity attenuation in transiting the slit of width w. We will return to this consideration below and show that it is readily resolved. In the meantime, as a matter of convenience, we choose arbitrary units with $W_{os}(0) = 1$.

Our present investigation also does not consider slits in the sub-wavelength range $w < \lambda$. Nevertheless, we will have need to consider slit widths in the neighborhood of $w \gtrsim \lambda$ where classic references such as that of Elmore and Heald caution us that "the Kirchhoff diffraction theory is less accurate, and it is expected that the single-slit diffraction factor will no longer give a good description of the envelope."[13] This caution is quite correct. However, we will return to this point and show that such deviations are not a factor in the essential criteria for duality violation. Accordingly, we proceed here with the use of the $sinc^2\alpha$ envelope in the interests of illustrating duality violation using an explicit analytical function for that envelope and, later in this section, we show that the essential criteria for duality violation are well satisfied in the present case and identify the general requirements of an arbitrary envelope in meeting these criteria.

From Eq. (22), we can write the expression for the output single slit probability

$$P_{os}(\alpha_t) = \int_{-\alpha_t}^{\alpha_t} sinc^2\ \alpha\ d\alpha \tag{24}$$

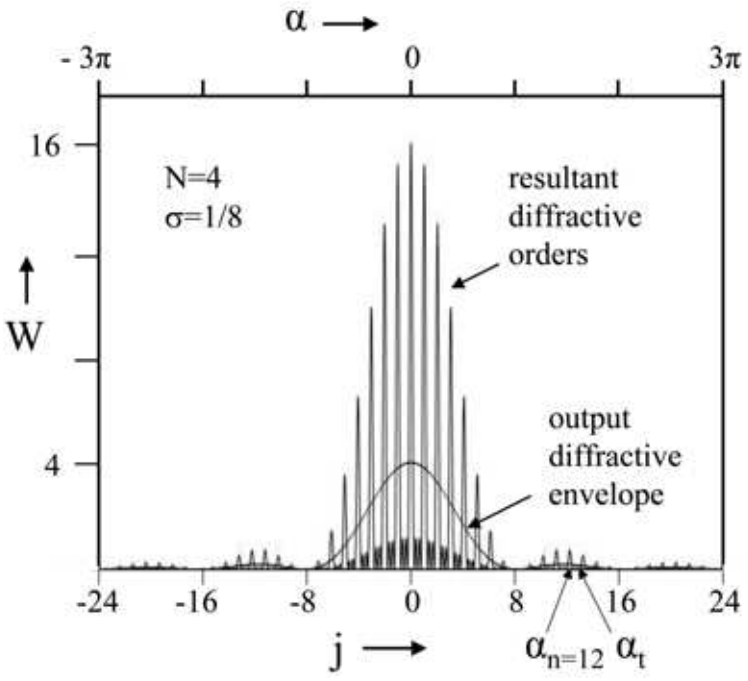

FIG. 3: Intensity plots in arbitrary units of the single-slit output diffractive envelope $sinc^2\alpha$ scaled by a factor N, the number of irradiated slits, to give a smoothly varying intensity envelope in α-space representing the collective output probability of the grating, and the diffractive order peaks representing the resultant probability. An untypically small $N = 4$ is chosen here for clarity of depiction. The integrals of the two intensity functions are essentially equal, demonstrating probability conservation for the $\sigma = 1/8$ approximation of dense sampling.

where envelope truncation

$$\alpha_t = \frac{\pi w}{\lambda} \tag{25}$$

found from Eq. (23) with $\theta = 90°$ provides the appropriate limits of the Eq. (24) integral. In analogy to the collective output probability of two beams incident on a beam splitter, the collective output probability of the grating is

$$P_{o;\sigma}(\alpha_t) = N \int_{-\alpha_t}^{\alpha_t} sinc^2\ \alpha\ d\alpha \tag{26}$$

where here, relative to $P_{os}(\alpha_t)$, the coefficient N is effectively the number of slits irradiated by the incident beam. N is well determined for a given beam incident beam diameter D, σ, and α_t. The $Nsinc^2\alpha$ intensity envelope is shown in Fig. 3. The Eq. (24) and Eq. (26) probabilities are identified as functions of the integration limit α_t. From Eq. (25) we see

that those probabilities are equivalently functions of w. Fig. 3 shows an example of an α_t for a narrow slit $w \gtrsim \lambda$. The truncation of the $sinc^2\alpha$ envelope by $\pm\alpha_t$ at this w results in a central lobe and partial side lobes as output from each slit with substantial envelope distribution from $+90°$ to $-90°$. Conversely, significantly increasing α_t results in a wide $w \gg \lambda$, adds multiple, greatly diminished side lobes to each slit output and concurrently confines the significant envelope contribution to the forward direction clustered about $0°$.

However, the Eq. (24) probability $P_{o;\sigma}(\alpha_t)$ computed in α-space, is clearly an increasing function of α_t, or equivalently, of w. This result is in conflict with the Eq. (20) w-independent probability $P_{o;\sigma}$ deduced from physical considerations for gratings of varying w but having some specific σ. The conflict can be understood by noting that the Eq. (24) dependence on w is an artifactual consequence of integrating the unscaled Eq. (22) intensity in α-space rather than in physical space over the θ angle azimuthal to the slit. This can be appreciated by examining the limit of large w for which the w-dependence of $P_{o;\sigma}(\alpha_t)$ becomes vanishingly small. In this limit, the significant contributions to the integral are entirely confined to small α where $\alpha = (\pi w/\lambda)\sin\theta \to \pi w\theta/\lambda$ and α in this range is linear in θ. Nevertheless, the Eq. (26) collective output probability will prove to be extremely useful precisely because of its w-dependence in α-space.

We next turn to the interference-generated resultant probability emerging from the intersecting individual slit output $sinc\ \alpha$ amplitude envelopes (shown in Fig. 2) that generate the output $sinc^2\alpha$ intensity envelopes. With the incident beam of some Gaussian diameter D spanning a large number N of grating slits, the non-null resultant probability computed in α-space is effectively confined to the sum of the individual integrals of the narrow, highly directional principal order intensity peaks, and the intermediate subsidiary peaks are vanishingly small.

The classic Kirchhoff expression for the resultant diffraction order intensity is given by

$$W_r(\alpha) = W_{os}(0) sinc^2\alpha \left(\frac{\sin(N\alpha/\sigma)}{\sin(\alpha/\sigma)}\right)^2 \tag{27}$$

where $W_{os}(0) = 1$ is, as before, the single slit intensity at $\alpha = 0$ set to unity. The quantity $(\sin(N\alpha/\sigma)/\sin(\alpha/\sigma))^2$ is the "grating factor". In this form, the diffraction peak maxima extend above the single slit $sinc^2\alpha$ intensity envelope but are proportional to it.

In the literature, Eq. (27) is generally modified by replacing $W_{os}(0)$ with the corresponding collective N slit intensity $W_o(0)$ at $\alpha = 0$ and inserting a compensating N^{-2} factor

based upon the justification that the N slit intensity at $\alpha = 0$, $W_o(0) = N^2 W_{os}(0)$. That modification would yield the familiar depiction of a diffraction envelope with the maxima of the diffraction order peaks in contact with that envelope. However, we deliberately omit that modification here in the interests of correctly tracking the relative probability in the output→resultant transition. Output quantities appropriately refer to pre-interference tabulations of those quantities. If the single slit output intensity is $W_{os}(0)$ at $\alpha = 0$, the collective output intensity from N slits is $NW_{os}(0)$. The same principle is involved with the Eq. (24) single slit output probability and the Eq. (26) collective output probability.

Consequently, the integral of the Eq. (22) single slit output scaled by N, i.e. $NW_{os}(\alpha)$, is correctly equal to the integrated Eq. (27) as depicted in Fig. 3. The computed equality of these integrals for any selected limits $\pm\alpha_t$ is a confirmation that probability is conserved in the output→resultant transition. Exact integral equality is achieved as $\sigma \to 0$ for which the sample density of the output envelope by the resultant orders becomes infinite. However, even the small but finite $\sigma = w/p = 1/8$ selected in Fig. 3 for illustrative clarity, gives an approximation of "dense sampling". In this approximation, integral equality is closely achieved as a function of the integration limits $\pm\alpha_t$ with only minor perturbations as those limits pass between discrete resultant orders such as the depicted α_t displaced from the $n = 12$ order.

Again, for purposes of illustrative clarity in Fig. 3, an $N = 4$ has been selected, which is lower than that for typical experimental conditions by about two orders of magnitude, so that the envelope and the diffraction order peaks can both be represented on the same scale. Low intensity secondary diffraction order peaks appearing near the bases of the principal diffraction order peaks in the figure diminish to negligible values for experimentally realistic large N.

The integral of the diffraction envelope, which gives the collective output probability in α-space, has limits $\pm\alpha_t$ where the envelope truncates at the physical azimuthal angles $\theta = \pm 90°$ relative to the grating normal. These limits are a function of w by $\alpha_t = w\pi/\lambda$. The narrow resultant peaks (principal maxima) arise from interference of the intersecting single-slit diffraction envelope amplitudes. The peaks occur at $\alpha = \alpha_j = j\pi\sigma$ which is $j\pi/8$ in the figure. The resultant probability can be expressed as a summation in α-space with limits $\pm\alpha_n$ where $|\alpha_n| \lesssim |\alpha_t|$. For small w, the grating is "fine", the limits in α-space are low and $w \gtrsim \lambda$. For $j = 12$, $\alpha_{12} = 3\pi/2$ and a grating with a truncation value marginally

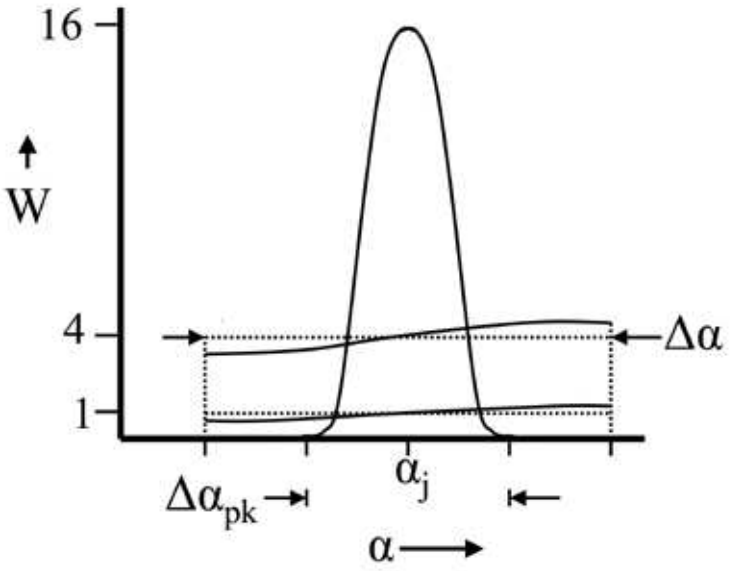

FIG. 4: A detail of a single subinterval of Fig. 3 with $N = 4$ and $\sigma = 1/8$ showing some arbitrary j^{th} peak, the associated single slit output intensity envelope and the collective (four) slit output intensity envelope with its associated Riemann approximation. The width of the subinterval is $\Delta\alpha = \pi\sigma$ and the width of the peak is $\Delta\alpha_{pk} = \pi\sigma/2$ for the present $N = 4$. Most critically, the figure depicts the probability equivalence of the peak and the collective output intensity envelope over the subinterval.

inclusive of the $\pm 12^{th}$ orders, i.e. $\alpha_t \gtrsim \alpha_{12}$, has $w \gtrsim 3\lambda/2$. Conversely, for large w (not shown in the figure), the grating is "coarse", the limits in α-space are high and $w \gg \lambda$.

Probability conservation in the output→resultant transition can also be assessed for individual resultant peaks. From Eq. (27), the grating factor separates the interference maxima into subintervals

$$\Delta\alpha = \pi\sigma \tag{28}$$

and, within those subintervals, the null to null peak base width is

$$\Delta\alpha_{pk} = 2\pi\sigma/N. \tag{29}$$

A detail of a subinterval is shown in Fig. 4. The total output probability for this subinterval

is

$$P_{oj;\sigma}(\alpha_j) = N \int_{\alpha_j - \Delta\alpha/2}^{\alpha_j + \Delta\alpha/2} sinc^2\alpha \; d\alpha$$
$$= N\pi\sigma \; sinc^2\alpha_j \tag{30}$$

where the area under the single slit $sinc^2\alpha$ curve at α_j is approximated by the product of $\Delta\alpha = \pi\sigma$ and the functional value $sinc^2\alpha_j$. (The value of α at the j^{th} order is $\alpha_j = j\pi\sigma$ where the applicable σ is implicit from the context.) The total subinterval output probability is given by that area, $\pi\sigma sinc^2\alpha_j$, multiplied by the number N of contributing slits. We are reminded again that this factor giving total output probability is linear in N since it relates to an accounting of the collective single slit probability outputs prior to the subsequent interference that yields the resultant probabilities. Total output probability in the earlier example of two beams incident on a beam splitter provides a useful analog. As a result of the linear factor N in Eq. (30), the collective output intensity envelope is appropriately depicted as the single slit output intensity envelope $sinc^2\alpha_j$ necessarily scaled up by a factor N as shown in Fig. 4. This scaling still leaves the resultant diffraction peak maxima above the collective output envelope but now graphically illustrates the essential conservation of probability in the output→resultant transition for this single resultant peak.

Conservation of probability can also be demonstrated quantitatively for this arbitrary single j^{th} resultant peak shown in Fig. 4. The probability for this peak is found from Eq. (27) noting that

$$\frac{\sin\left(N\alpha_j/\sigma\right)}{\sin(\alpha_j/\sigma)} = N$$

at the principal maxima $\alpha = \alpha_j$. Then

$$P_{rj;\sigma}(\alpha_j) = \int_{\alpha_j - \Delta\alpha_{pk}/2}^{\alpha_j + \Delta\alpha_{pk}/2} sinc^2\alpha \; \left(\frac{\sin\left(N\alpha/\sigma\right)}{\sin(\alpha/\sigma)}\right)^2 d\alpha$$
$$= \left(\frac{1}{2}\right)\left(\frac{2\pi\sigma}{N}\right)\left(N^2 sinc^2\alpha_j\right)$$
$$= N\pi\sigma \; sinc^2\alpha_j \tag{31}$$

where the integral of the j^{th} peak is readily evaluated by noting that, because of peak symmetry about $\alpha_j \pm \pi\sigma/2N$, the peak occupies one-half of the rectangular area defined by the peak null to null base width $\Delta\alpha_{pk} = 2\pi\sigma/N$ and magnitude $N^2 sinc^2\alpha_j$. Those factors

resolve to a resultant subinterval probability and an output subinterval probability, both of which can be equated to a Riemann-approximated subinterval area, i.e.

$$P_{rj;\sigma}(\alpha_j) = P_{oj;\sigma}(\alpha_j) = \pi\sigma(N sinc^2\alpha_j). \tag{32}$$

Accordingly, over all α-space we can define the total resultant probability as a Riemann sum

$$P_{r;\sigma}(\alpha_n) = \sum_{j=-n}^{n} \pi\sigma(N sinc^2\alpha_j) \tag{33}$$

and the total output probability as the corresponding definite integral

$$P_o(\alpha_t) = \int_{-\alpha_t}^{\alpha_t} N sinc^2\alpha_j \, d\alpha \tag{34}$$

where $\Delta\alpha = \pi\sigma \to d\alpha$. We have limit equivalence $\alpha_n = \alpha_t$ in Eqs. (33-34) when $\alpha_t = n\pi\sigma$. We can temporarily defer consideration of deviations of the continuous-valued α_t variable from the discrete-valued α_n variable since we are currently imposing dense sampling in α-space. Dense sampling divides the integration partition into a large number of subintervals ($n \gg 1$). Consequently, $\alpha_t > \alpha_n$ results in fractional integration of Eq. (34) into the $\pm(n+1)$ subintervals not included in the Eq. (33) summation. The contribution of those two fractionally integrated subintervals relative to that of the total $2n+1$ subintervals partition is vanishingly small.

As a formal matter, in the dense sampling limit $\sigma \to 0$, the partition subinterval $\Delta\alpha \to 0$ which gives $n \to \infty$ and

$$\lim_{n\to\infty} \sum_{j=-n}^{n} \Delta\alpha \; sinc^2 \; \alpha_j = \int_{-\alpha_t}^{\alpha_t} sinc^2 \; \alpha \; d\alpha \tag{35}$$

where the integration limits $\pm\alpha_t$ are applicable since $\alpha_n \to \alpha_t$. The limit condition in Eq. (35) is recognized as the Riemann sum equivalency to the definite integral on the right. Ultimately, the Riemann sum serves as a mathematical intermediary that demonstrates output$\to$resultant probability equivalency when $\alpha_n \to \alpha_t$.

Nevertheless, despite their equivalency, the α-space quantities $P_o(\alpha_t)$ and $P_{r;\sigma}(\alpha_n)$ are not satisfactory expressions of probabilities since an examination of output probability for some fixed σ predicts w-independence. Both $P_o(\alpha_t)$ and $P_{r;\sigma}(\alpha_n)$ are clearly increasing functions of w through their respective w-dependent respective limits α_t and α_n. However, because of the relative equality of $P_o(\alpha_t)$ and $P_{r;\sigma}(\alpha_n)$, the w-dependence of $P_{r;\sigma}(\alpha_n)$ can be removed

by normalization with $P_o(\alpha_t)$ which has the same w-dependence. The normalized resultant probability

$$P_{r;\sigma}(\alpha_t) = \frac{\sum_{j=-n}^{n} \pi\sigma \; sinc^2\alpha_j}{\int_{-\alpha_t}^{\alpha_t} sinc^2\alpha_j \; d\alpha}$$
$$= 1 \tag{36}$$

gives a w-independent constant to within a vanishingly small discrepancy arising from $\alpha_t > \alpha_n$ as discussed above.

The summation limits $\pm n$ are set by the condition $|\alpha_n| \leq |\alpha_t|$. Note that the identification of the Eq. (36) normalized expression $P_{r;\sigma}(\alpha_t)$ differs from that of the Eq. (33) unnormalized expression $P_{r;\sigma}(\alpha_n)$ only with regard to the α-space limits. The summation in $P_{r;\sigma}(\alpha_t)$ has the same $\pm n$ limits as that of $P_{r;\sigma}(\alpha_n)$ but the more distal integration limits $|\alpha_t| \geq |\alpha_n|$ of the Eq. (34) normalization integral sets α_t as the defining functional variable of Eq. (36). Because of dense sampling, Eq. (36) is very nearly a constant and, as such, is effectively independent of α_t. However, as a formality we retain α_t as an apparent functional dependent. (Since $\alpha_t = \pi w/\lambda$, α_t-invariance is equivalent to w-invariance for Eq. (36) where λ is a constant.)

From a purely pragmatic viewpoint, the normalization in Eq. (36) expeditiously achieves the required w-invariance of $P_{r;\sigma}(\alpha_t)$ for the class of gratings with dense sampling. More significantly, however, the Eq. (36) normalization of relative resultant probability by relative output probability (distinct from PIQM normalization, Section I) is fundamental in quantifying any probability non-conservation in the output→resultant transition. For separate real entities of energy quanta and probability, the constant proportionality required by PIQM duality is no longer a constraint. In LRQM, deviations from duality may occur as non-conservation of probability manifested as a change in the ratio of the resultant probability relative to the output probability. Therefore, for a mechanism that potentially achieves duality violation by probability non-conservation in some transition process such as grating output→resultant, it is critical to represent that resultant probability relative to the base output probability in order to express that non-conservation.

Non-conservation of probability is, however, not in evidence as $\sigma \to 0$ provides dense sampling of the outputs by the resultants. Then the Eq. (36) normalized form $P_{r;\sigma}(\alpha_t)$ rectifies the artifactual increase of the Eq. (33) $P_{r;\sigma}(\alpha_n)$ with w and provides the physical probability as a function of α_t, albeit a trivially constant unit value.

In analogy to the beam splitter with two incident beams, we again have conservation of probability in the output→resultant transition and we also have spatial regions of null resultant probability and regions of "amplified" resultant probability. Similarly, the manifestation of these resultant probabilities does not alter the reality of the output probability wave structures. The grating, however, differs from the beam splitter in that the origin of the resultants is physically displaced from the grating surface but still in the near field where the emergent expanding individual slit output envelopes begin to intersect and interfere as shown in Fig. 2.

To complete the analysis of the grating with dense sampling, we need to also assess energy in the output→resultant transition. As the expanding output probability envelopes interfere, the resident energy quanta transfer without loss onto the forming resultant diffraction order beams. The process is purely an energy quanta transfer. No wave entity is transferred in a process analogous to that of energy quanta transfer at a beam splitter. The consequent continued proportionality of total energy and probability in the output→resultant transition yields a constant Ω throughout,

$$\Omega_i = \frac{E_i}{P_i} = \Omega_o = \frac{E_o}{P_o} = \Omega_r = \frac{E_r}{P_r} = 1. \tag{37}$$

We note that in the Eq. (36) $P_{r;\sigma}(\alpha_t)$ expression, the property of dense sampling is critical to maintaining an $\Omega_r = 1$ independent of w. As α_t $(= \pi w/\lambda)$ is increased, the normalization integral monotonically increases whereas the summation abruptly increases with two additional final terms $\pm n' = \pm\,|n+1|$ as α_t reaches a value corresponding to a new $j = n'$ order. Nevertheless, for dense sampling, the additional $\pm n'$ terms are incrementally small relative to the existing sum of the $2n+1$ terms..

B. Gratings with sparse sampling

The dependence upon dense sampling for the maintenance of $\Omega \approx 1$ suggests that the converse, i.e. "sparse" sampling, constitutes a potential mechanism for achieving significant deviations of Ω from unity which is equivalently a violation of PIQM duality. Specifically, we examine $\sigma = 0.5$, characteristic of Ronchi rulings. This ratio σ is notable in that the side lobes of the output probability are each entirely expressed by the single, odd order that bifurcates those lobes in α-space as shown in Fig. 5. This is a significant fortuitous property

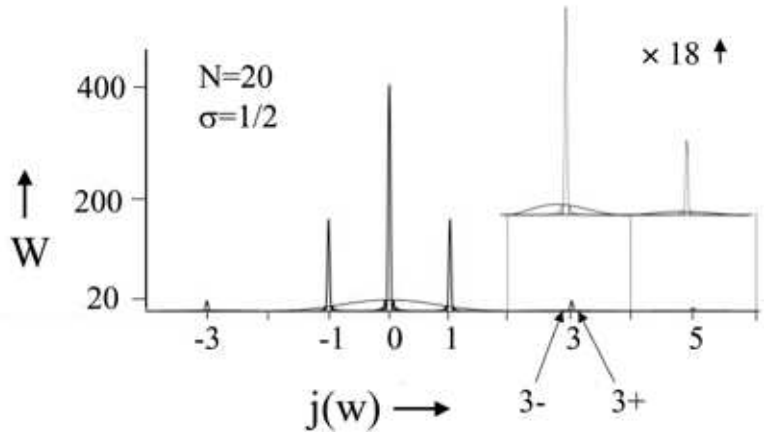

FIG. 5: A $\sigma = 0.5$ sparse sampling analog to the dense sampling approximation shown in Fig. 3. Odd j peaks for $j \geq 3$ have probabilities that fully express the probability of the collective output lobe that they respectively bifurcate.

of a $\sigma = 0.5$ grating attributable to the non-expression by the null-valued even orders on either end of each of those lobes. It reflects a corollary of Eq. (36) that it is necessarily the non-null resultants that express the outputs. The probability for $\sigma = 0.5$,

$$P_{r;0.5}(\alpha_t) = \frac{(\pi/2)\sum_{j=-n}^{n} sinc^2\ \alpha_j}{\int_{-\alpha_t}^{\alpha_t} sinc^2\ \alpha\ d\alpha}, \tag{38}$$

is merely a special case of the Eq. (36) probability where we again consider $w \gtrsim \lambda$ (fine gratings) to $w \gg \lambda$ (coarse gratings). Similarly,

$$P_{rj;0.5}(\alpha_t) = \frac{(\pi/2)sinc^2\ \alpha_j}{\int_{-\alpha_t}^{\alpha_t} sinc^2\ \alpha\ d\alpha} \tag{39}$$

for the j^{th} order probability.

However, for the sparse sampling associated with $\sigma = 0.5$,

$$\alpha_j = j\pi/2 \tag{40}$$

and the Eq. (38) probability, unlike the Eq. (36) probability with $\sigma \to 0$, is no longer a constant of the functional variable α_t. The deviations from constancy occur as α_t approaches the neighborhood of the odd orders. Eq. (38) is plotted in Fig. 6 in α_t-space from $\alpha_t = \pi$ to 3π. For $\alpha_t = \pi$, truncation occurs at the $\pm 2^{nd}$ orders, representing a relatively fine grating, whereas $\alpha_t = 3\pi$ corresponds to truncation at the $\pm 6^{th}$ orders and the grating is modestly

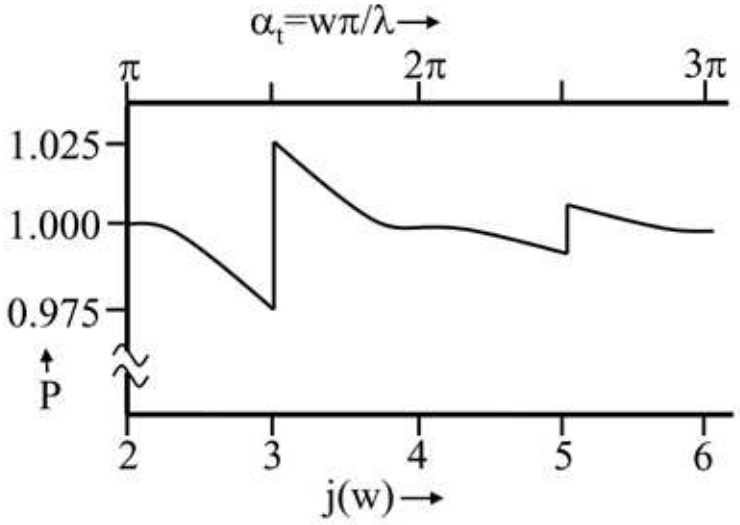

FIG. 6: Resultant probability $P_{r;0.5}(\alpha_t)$ plotted here for positive α_t since functional evaluation of the probability at limits $\alpha_t = \pm w\pi/\lambda$ is understood. The excursions from unity represent measurable non-conservation of probability. These excursions are notable for a grating that has a w for which α_t is in the neighborhood of $\alpha_{j=3}$.

coarser. The horizontal axis on the figure shows only positive values since symmetry ensures that any choice of α_t automatically sets integration limits of $\pm\alpha_t$ and concurrently sets summation limits $\pm n$ in the evaluation of $P_{r;0.5}(\alpha_t)$.

An examination of Fig. 6 notably shows a probability edge transition of $\sim 5\%$ for α_t in the neighborhood of the $\pm 3^{rd}$ orders. The transitions at the odd orders diminish in magnitude as α_t increases further, ultimately yielding flat-line constancy of $P_{r;0.5}(\alpha_t)$ for very large α_t (coarse) gratings.

The functional structure of the Fig. 6 probability is, of course, simply a consequence of the sparse sampling of the $\sigma = 0.5$ gratings. As α_t at $\alpha_{j=2}$ ($\pm 2^{nd}$ order) is increased, the $P_{r;0.5}(\alpha_t)$ summation is constant whereas the normalization integral increases resulting in a maximum $\sim 2.5\%$ decrease in the limit as α_t approaches $\alpha_{j=3}$ from the left. At $\alpha_{j=3}$, $P_{r;0.5}(\alpha_3)$ discontinuously increases by $\sim 5\%$ with the inclusion of the $j = \pm 3^{rd}$ terms in the summation. As α_t is increased toward $\alpha_{j=4}$, the summation with end terms at $j = \pm n = \pm 3$, is again constant while the normalization integral continues to increase resulting in a return to the probability value at $j = 2$. This functional behavior repeats with increasing α_t but with progressively diminishing discontinuities at the odd j. (Since the resultant beams

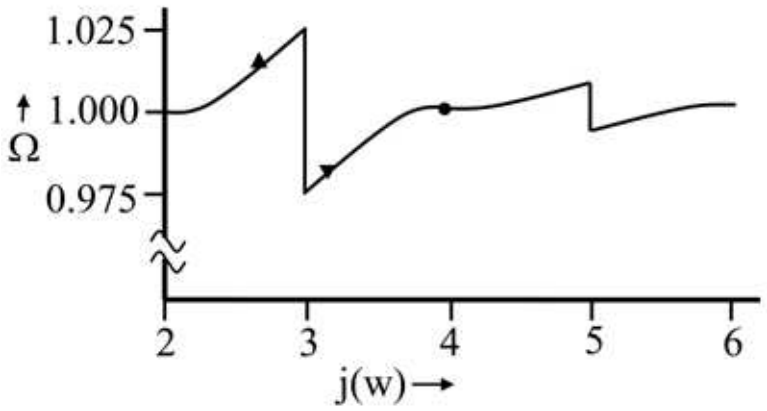

FIG. 7: Theoretical occupation value $\Omega_{r;0.5}(\alpha_t) = \Omega_{G[j(w)]\ th}$ for $\sigma = 0.5$. With energy E set to unit value, this function is the inverse of that in Fig. 6. The regions above the unity level identify grating w-values that give enrichment whereas those regions below unity correspondingly are associated with depletion. The three experimentally measured $\Omega's$ are plotted for comparison on this theoretical curve at their respective j-equivalent values of truncation: $\Omega_{G(2.63)\ ex}$ as ▲, $\Omega_{G(3.16)\ ex}$ as ▼, and $\Omega_{G(3.94)\ ex}$ as •.

are physically narrow but finite in Gaussian diameter, $P_{r;0.5}(\alpha_t)$ only approximates a true mathematical discontinuity at odd j.) The convergence of $P_{r;0.5}(\alpha_t)$ to a constant, unit value in the limit as $\alpha_t \to \infty$ verifies that the Eq. (38) probability is properly scaled.

Then upon inspection of Fig. 6, we conclude that probability is annihilated in the output→resultant transition for $\sigma = 0.5$ gratings with $\alpha_t \lesssim \alpha_j$ at odd j. Conversely, probability is created in the output→resultant transition for $\sigma = 0.5$ gratings with $\alpha_t \gtrsim \alpha_j$ at odd j.

As in the above case of α_t and α_j, we have applied a convention in which truncation-related quantities are associated with a resultant j^{th} diffraction order. It will frequently be convenient to return to this convention. For our purposes here, this association is made with a positive-valued j but by symmetry the association also applies to the corresponding negative-valued j (with, of course, a reversal in the above inequalities).

We proceed with an examination of the Eq. (38) probability by computing the associated

occupation value for this class of gratings,

$$\Omega_{r;0.5}(\alpha_t) = \frac{E_{r;0.5}(\alpha_t)}{P_{r;0.5}(\alpha_t)} = \frac{\int_{-\alpha_t}^{\alpha_t} sinc^2\ \alpha\ d\alpha}{(\pi/2)\sum_{j=-n}^{n} sinc^2\ \alpha_j} \tag{41}$$

since the output energy, which can be set to unity, is conserved in the transition to resultant energy, $E_o = 1 = E_{r;0.5}$. Functionally, $\Omega_{r;0.5}(\alpha_t)$ plotted in Fig. 7, is the inverse of the Fig. 6 probability $P_{r;0.5}(\alpha_t)$. $\Omega_{r;0.5}(\alpha_t)$ then also converges to unity as $\alpha_t \to \infty$. For $\sigma = 0.5$ gratings with $\alpha_t \lesssim \alpha_j$ at odd j, we have enrichment of the resultant diffraction orders. Conversely, for $\sigma = 0.5$ gratings with $\alpha_t \gtrsim \alpha_j$ at odd j, those orders are depleted.

It is instructive at this juncture to detail the respective diffraction order parameters P, E, and Ω for a pair of Ronchi gratings identified as $G(3\pm)$ that have truncation on either side of the significant $\pm 3^{rd}$ orders. Care should be taken to avoid confusion of these two $\pm$ designations. For $G(3-)$, the positive-valued α-space truncation is denoted as $\alpha_{3-} = \alpha_t \lessapprox \alpha_3$, which marginally excludes the formation of the $\pm 3^{rd}$ order resultant probability channels by locating $+\alpha_t$ at the "interior" (left) null at the base of the $+3^{rd}$ order peak. By symmetry, the negative-valued $-\alpha_t$ is situated at the interior (right) null of the -3^{rd} order peak. Similarly, for $G(3+)$ the positive-valued α-space truncation is denoted as $\alpha_{3+} = \alpha_t \gtrapprox \alpha_3$, which marginally allows the formation of the $\pm 3^{rd}$ order resultant probability channels at threshold by situating $\pm\alpha_t$ at the respective exterior nulls of the $\pm 3^{rd}$ order peaks. For a given operating wavelength λ, the two Ronchi gratings $G(3\pm)$ are characterized entirely by their respective slit widths $w_{3\pm}$. From Eqs. (25) and (40) at the $+3^{rd}$ order threshold the requisite width is $w_3 = 3\lambda/2$. Therefore the gratings $G(3-)$ and $G(3+)$ have respective widths $w_{3-} \lessapprox 3\lambda/2$ and $w_{3+} \gtrapprox 3\lambda/2$.

Note that in the above quantities, we have extended the convention of referencing truncation to a j^{th} order by use of $j-$ to indicate marginal truncation exclusion of the $\pm j^{th}$ orders and $j+$ to indicate marginal truncation inclusion of the $\pm j^{th}$ orders.

The P, E, and Ω parameters for these two gratings $G(3\pm)$ are shown in Fig. 8 where the collective and the individual j^{th} probabilities are computed from Eqs. (38) and (39), respectively. The output energy $E_o = 1$ is conserved giving a total of $E_r = 1$ distributed onto the propagating orders as E_{rj}. Consistent with probability as a relative quantity, these E_{rj} are found from the ratio of the Eq. (39) individual j^{th} order resultant probability

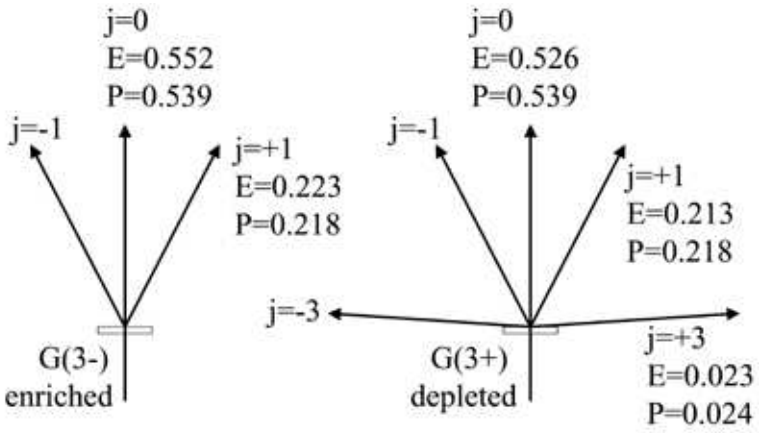

FIG. 8: Tabulation of energy and probability values on the resultant propagating orders for gratings $G(3-)$ and $G(3+)$ where the total energy is unit valued. By symmetry, values on $\pm j$ are the same for both gratings.

$P_{rj;0.5}(\alpha_t)$ and the Eq. (38) collective resultant probability $P_{r;0.5}(\alpha_t)$. The Fig. 8 example illustrates the essential features of probability non-conservation and energy distribution in the neighborhood of the $\pm 3^{rd}$ order threshold probability discontinuity.

We note that since this discontinuity alters the proportionality of the wave-like probability and the particle-like energy, the phenomenon can be expressed as a "duality modulation". In the Fig. 8 example, the $G(3-)$ grating with $\pm\alpha_{3-}$ truncation points provides a $+2.5\%$ duality modulation upon comparing the $G(3-)$ occupation value $\Omega_{G(3-)}$ to the ordinary value $\Omega = 1$. Similarly, $G(3+)$ provides a -2.5% duality modulation.

Most generally, this phenomenon of duality modulation is potentially applicable to any (fine) grating that yields a small number of resultant orders for which one or two can be located near or just beyond the plane of the grating "at threshold". In other words, the precise shape of the output diffraction envelope is not a critical factor. This can be understood by the relationship of the diffraction envelope and the interference factor that modulates that envelope. Within any single subinterval, the j^{th} peak arises from the same interference factor, identified earlier in Eq. (31), modulating a value $f(\alpha_j)$ of an output diffraction envelope $f(\alpha)$ in place of $sinc^2\alpha$. Similarly, in the present context of the regular Ronchi grating where $w \gtrsim \lambda$, the departure from the Fraunhofer approximation $w \gg \lambda$ gives a single slit output intensity envelope that is not precisely expressed by $sinc^2\alpha$. However,

orders near threshold for gratings with sparse sampling are still predicted to give probability non-conservation.

It may be appreciated at this point that the existence of expressed resultant probability discontinuities for fine, sparsely sampled gratings could have been deduced directly and quite succinctly from basic LRQM principles. The essential rationale for such a deduction is derived from the observation that, for a set of gratings with a common sparse sampling, e.g. $\sigma \sim 0.5$, all such gratings have the same output probability, but we can always identify specific pairs of these gratings with nearly identical slit widths w_{j+} and w_{j-} for which w_{j+} marginally admits a significant resultant order near threshold and w_{j-} marginally blocks that order. For these two gratings considered in succession, the collective resultant probability must exhibit an abrupt decrease in the near infinitesimal $w_{j+} \rightarrow w_{j-}$ transition. That abrupt decrease does not occur for the smoothly varying output probability. Similarly, the output energy is also unaltered by that transition. Therefore, in the absence of an energy-dissipative mechanism, the distribution of the output energy onto the resultants yields a relative enrichment of the w_{j+} resultants with respect to the w_{j-} resultants. However, without the basis developed in the previous subsection for densely sampled gratings, the assessment of occupancy in threshold transitions is limited to relative changes in occupancy. Moreover, the occupancy is not characterized outside the neighborhood of the w_j threshold value.

Accordingly, we have proceeded here in a less succinct manner by first examining elementary beam splitter configurations to elucidate the basic principles of probability conservation from the perspective of LRQM. We then examined resultant probability associated with gratings having dense sampling in order to develop a generalized functional expression applicable to all gratings that characterizes resultant probability over the full α-space and not just in the neighborhood of threshold transitions before proceeding to an examination of gratings having sparse sampling.

It is of some peripheral interest that the spatial physical discreteness of resultant diffraction orders of a grating is the essential property that produces duality modulation in the present example. We recall that it was also spatial physical discreteness that yielded duality modulation for the case of a discrete photon beam incident on a beam splitter. For a grating, it is the discrete increment of probability (on a highly directional diffraction order) that modulates duality whereas for the beam splitter, it is the discrete increment of energy

that produces this modulation.

We conclude this section on the theoretical basis for duality violation with a brief but relevant examination of grating anomalies. This examination is necessitated by some apparent similarities of those anomalies to the phenomena considered here.

Grating anomalies, since their discovery by Wood in 1902, have continued to be a subject of intensive experimental and theoretical investigation.[14] These anomalies are deviations, often abrupt, in the diffraction order irradiances as a function of a parameter such as wavelength. These deviations were initially designated as anomalies since they departed from predictions of earlier classical principles thought to fully characterize grating phenomena. Their continued characterization as "anomalies" is now generally regarded as a misnomer since sophisticated theoretical electromagnetic analyses of these phenomena have substantially approximated the experimental observations.

Our particular interest here concerns "Rayleigh" anomalies that have a theoretical basis postulated by Lord Rayleigh several years after their discovery by Wood.[15] Rayleigh anomalies are characterized by abrupt increases in the irradiance of propagating orders as one of those orders "at threshold" near the grating plane is extinguished by an incremental wavelength increase. The essential theoretical basis postulated by Lord Rayleigh consists of coherent (photon) scattering of the threshold order on a grating's periodic structures. By interference, the scattered threshold order (inclusive of its irradiance) is coherently redistributed onto the remaining propagating orders in proportion to the relative intensities of those orders. This coherent scattering process is fully consistent with PIQM which was developed two decades later. The postulated theoretical basis transfers photon energy quanta as well as photon wave probabilities to the remaining propagating orders thereby maintaining duality.

We seek here an alternative demonstration in LRQM of Rayleigh-like anomalies in the absence of the coherent scattering process postulated by Lord Rayleigh. With $\sigma = 0.5$, the slit width w is selected as the dependent parameter consistent with our previous analysis. From Eq. (25), for which w and λ are inversely related, LRQM predicts abrupt irradiance increases as orders reach threshold with progressive incremental decreases in w.

In the open interval between any successive $j = n$ and $j + 1$, each of the individual $2j + 1$ propagating orders exhibits a proportionately decreasing probability across that interval as shown in Eq. (39) and Fig. 6. (As in the Sec. 3 analysis, we consider the positive orders,

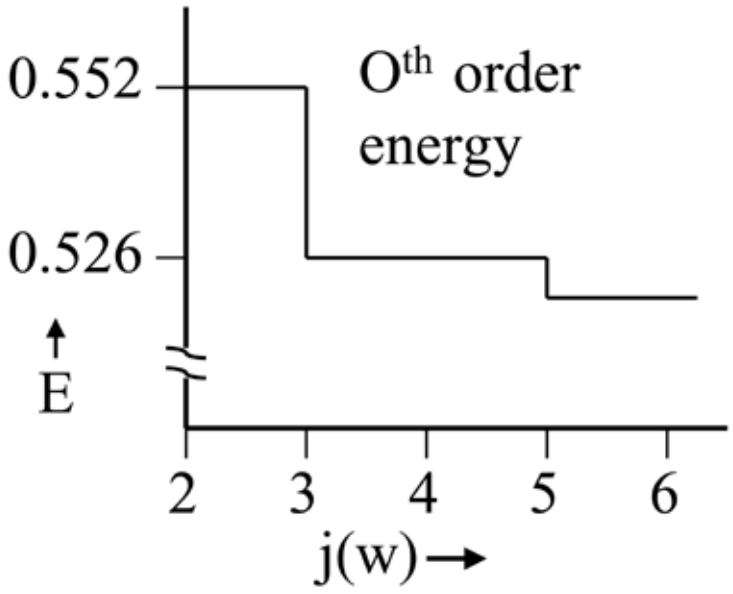

FIG. 9: 0^{th} order energy as a function of $j(w)$-equivalent truncation showing characteristic edge drops in propagating energy (or irradiance) associated with Rayleigh anomalies at threshold values of significant orders. Compare to Fig. 8.

but the corresponding negative orders are inclusive by symmetry for normal incidence.) The resultant probability of any single order relative to the total resultant probability Eq. (38) is constant for any α_t within any such open interval. This fractional resultant probability for the 0^{th} order

$$\begin{aligned} R_0(\alpha_t) &= \frac{P_{r0;0.5}(\alpha_t)}{P_{r;0.5}(\alpha_t)} \\ &= \frac{1}{\sum_{j=-n}^{n} sinc^2\, \alpha_j} \\ &= R_0(\alpha_n). \end{aligned} \tag{42}$$

is found from the ratio of Eq. (39) with $j = 0$ and Eq. (38). The independence of this ratio with respect to the α-space location α_t is emphasized by that ratio's equivalence to evaluation at the initial α-space location α_n of that interval, i.e. $R_0(\alpha_n)$. Essentially, the 0^{th} order's fractional share of the total resultant probability is calculated with respect to the probability of all propagating orders as a function of increasing α_t. This fractional share is a step function, constant for some total number of propagating orders $2n + 1$ and then discontinuously dropping as α_t reaches the next order at some $j = n + 1$. The 0^{th} order's

fractional share, calculated against the total probability of the $2(n+1)+1$ propagating orders, drops because of the additional probability on the $\pm|n+1|$ orders. Fig. 9 shows a plot of the 0^{th} order fractional share $R_0(\alpha_t)$.

In LRQM, energy quanta entering a probability field equilibrate onto that field in proportion to relative probabilities. Since the total output energy quanta in that field are independent of α_t, the 0^{th} order's fractional share of total resultant probability $R_0(\alpha_t)$ also gives the fraction of the total output energy E_o quanta equilibrating to the 0^{th} order. Then the energy on the 0^{th} order is

$$E_{r0} = E_o R_0(\alpha_t) \tag{43}$$

and with $E_o = 1$ in arbitrary units, E_{r0} is simply represented by the Fig. 9 $R_0(\alpha_t)$ step function. This function predicts the abrupt step-wise increases associated with Rayleigh anomalies both with regard to their locations at threshold α_t and their magnitudes relative to the irradiance of the paired extinguished threshold orders.

However, unlike the (PIQM-consistent) coherent scattering process postulated by Lord Rayleigh, the LRQM-consistent basis described earlier in this section also predicts a duality violation as quanta transfer from an extinguished threshold order to the remaining propagating orders without concurrently transferring wave intensity to those orders.

We stress that this finding does not preclude the existence of PIQM-consistent postulated coherent scattering as the operant mechanism for Rayleigh anomalies in other gratings and beam configurations, but it does expand the potential mechanisms that may be the cause of observed anomalies to include those that are not consistent with PIQM. In this regard we note that Lord Rayleigh based his theoretical analysis on experimental evidence from reflective gratings having deep, pronounced periodic groove structures which would be expected to exhibit significant scattering of a threshold order into the field of the remaining propagating orders. Conversely, the transmissive gratings we consider here consist of periodic flat opaque bands of negligible thickness that would not provide a comparable scattering mechanism.

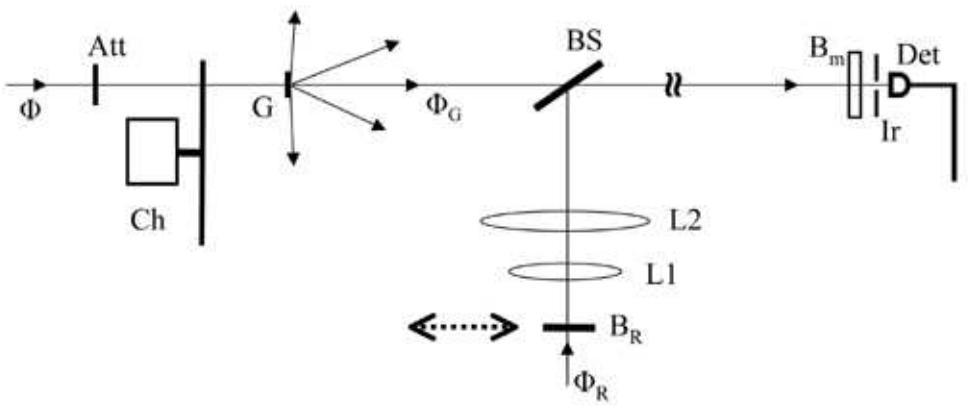

FIG. 10: Experimental apparatus configuration showing a potentially duality-modulated beam Φ_G following passage through a particular grating G. Φ_G is coupled to an ordinary beam Φ_R along a coupling path extending from a beam splitter BS. Coupling occurs with beam blocker B_R shifted to transmit Φ_R.

IV. EXPERIMENT

A. Apparatus and beam parameters

In this subsection we begin with a description of the experimental configuration shown in Fig. 10 before proceeding in subsequent subsections to the methodology for assessing duality violation on that configuration.

A HeNe laser generates a horizontally linearly polarized beam Φ of several milliwatts at 633 nm. Beam Φ traverses a variable attenuator Att and an optical beam chopper wheel Ch. Φ is normally incident on a grating G. The grating is one of several Ronchi rulings with various grating slit widths. The intervening opaque bands of the gratings defining those slits are 150 nm-thick reflective chromium deposited on a glass substrate. The particular grating under study is mounted with the ruling on the exit face and the bands vertically oriented. The 0^{th} order diffraction beam identified as Φ_G is incident on a 50:50 beam splitter BS. An independent, HeNe laser generates a horizontally linearly polarized beam Φ_R initially several milliwatts in power. Φ_R passes a retractable beam blocker B_R and enters a beam expander, $L1$ ($f = +100\ mm$) and $L2$ ($f = +200\ mm$), before forming a beamspot concentric with that of Φ_G on the beam splitter BS as shown in the Fig. 11 detail. This concentricity is a

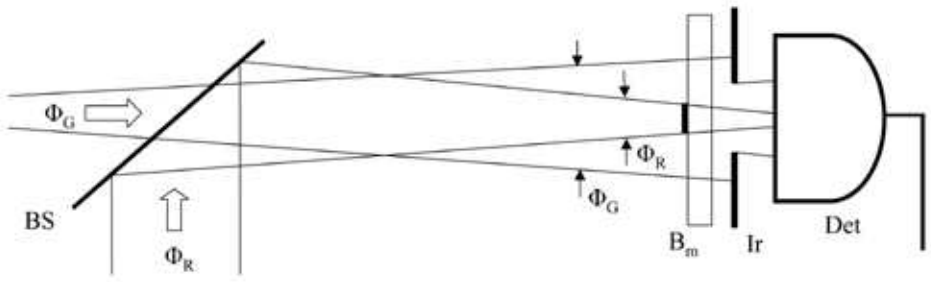

FIG. 11: Detail of Fig. 10 coupling path showing the substantial separation of Φ_R from Φ_G at the path terminus by convergence of the former onto a disk mask.

critical alignment for the apparatus. As a practical matter, the experimental configuration includes a number of beam directors not shown in Fig. 10 that facilitate beam alignment and folding of optical paths.

As we shall see in the subsequent subsections, measurement of duality violation imposes some general criteria on the beam and apparatus parameters. However, in the interests of facilitating replication of the present experiment, we provide specific parameters here in greater detail than that necessitated by the general criteria.

The (Gaussian) diameter of Φ_G at BS is $\sim 2mm$ by natural divergence from the source laser and whereas the corresponding diameter of Φ_R at BS is $\sim 4mm$ as a result of $L1$ and $L2$. The beam components exiting BS utilized here are the transmitted component of Φ_G and the reflected component of Φ_R. The orientation of BS is adjusted to coaxially align the Φ_R beam spot to the Φ_G beam spot at the terminus of a $2000mm$ "coupling path". This critical, second coaxial beamspot alignment effectively coaxially aligns the Φ_R and Φ_G beams on the coupling path. The variable attenuator Att significantly reduces the beam power of Φ such that Φ_G along the coupling path is $\sim 6\mu W$. The corresponding beam power of Φ_R along the coupling path is approximately two orders of magnitude higher at $\sim 600\mu W$. Φ_G expands to a Gaussian diameter of $\sim 4.5mm$ at the terminus of the coupling path by natural divergence from the emitting laser whereas Φ_R converges to $\lesssim 1.7mm$ by setting the relative spacing of lenses $L1$ and $L2$.

An assembly of a beam blocker B_m, an iris diaphragm Ir, and a photodiode detector Det is located at the coupling path terminus. B_m consists of a $1.7mm$ opaque disk mask mounted on a transparent glass substrate. The iris is set to a $3.3mm$ diameter. Beam

directors on the coupling path (not shown in Figs. 10 and 11) are used to provide concentric alignment of Φ_G and Φ_R with B_m and Ir. These settings collimate the $\sim 6\mu W$ Φ_G beam on the coupling path to an annular beam of $\sim 2.4\mu W$ incident on the adjacent detector Det. Of the remaining power, $\sim 1.5\mu W$ (25%) is blocked by the disk mask B_m and $\sim 2.1\mu W$ (35%) is blocked by the diaphragm of Ir. The $\sim 600\mu W$ power of Φ_R on the coupling path is blocked almost entirely by B_m alone leaving a residual $\sim 2.5\mu W$ incident on the detector. The function of the iris setting is to simultaneously restrict the radial sampling of Φ_G to an annular region closely coupled to Φ_R while concurrently providing adequate Φ_G power for detector measurement.

B. Observation of duality violation

We briefly digress in this subsection from the experimental apparatus and consider the theoretical basis for observing duality violation. As we discussed in Section III, orders passing to threshold for particular gratings are associated with abrupt redistributions of irradiance onto the remaining propagating orders for Rayleigh anomalies. A similar redistribution is predicted here for particular Ronchi gratings but, additionally, with the predicted phenomenon of duality violation on those remaining propagating orders. Consequently, for these Ronchi gratings the duality state of the propagating orders must be measured in order to establish whether those orders are ordinary, as would be expected for Rayleigh anomalies, or are in fact duality modulated. The experimental design used to achieve this measurement requires a transient coupling between a resultant presumptively duality-violating beam from the grating (a propagating order) and an independent ordinary beam.[6]

This design is analogous to the intersecting of two independent beams as used in numerous investigations [16] to experimentally assess duality violation by determining the presence or absence of interference between those beams, i.e. to provide a test of PIQM. A review of these investigations is given by Paul.[17] An observation of interference would seemingly violate Dirac's dictum that a photon (in PIQM) can interfere only with itself.[18]

The outcomes of these numerous investigations are conclusive demonstrations that interference does occur in apparent contradiction to PIQM. However, in a theoretical analysis of this phenomenon, Mandel makes the critical argument that for any given photon measured in the interference we do not know on which beam that photon had initially resided.[19]

Because of that lack of knowledge, each photon is treated in Mandel's analysis as interfering with itself. Consequently, interference in the intersection of independent beams is consistent with PIQM and does not provide a test of that interpretation. Concurrently, that interference is trivially consistent with LRQM.

In a variant of those independent beam investigations, we prepare one of the beams by transmission through a particular grating where we have some basis that a prepared beam Φ_G may specifically violate PIQM duality, i.e. the beam is in a depleted or enriched state from the perspective of LRQM but is necessarily ordinary for PIQM. Spatially transient equilibration of that prepared beam with a second, ordinary beam Φ_R by mutual interference over the coupling path should then yield a net transfer of energy quanta for LRQM but not for PIQM. That net energy transfer relative to Φ_G is readily measurable in the cw regime by detecting disparate beam powers on the sampled Φ_G with and without Φ_R present on the coupling path.

C. Gratings

The particular gratings used in the experiment are based upon the theoretical analysis presented in Section III. In the apparatus shown in Fig. 10, the horizontally linearly polarized ($\lambda = 633nm$) Φ is normally incident on one of three Ronchi transmission gratings G with respective slit widths w that are theoretically predicted to generate resultant orders that are respectively enriched, depleted and ordinary. For whichever of the three gratings is installed in the Fig. 10 apparatus, the lines on the exit face of that particular grating are vertically oriented thereby providing TM (S) polarization with respect to G in the usual classical configuration for observing grating anomalies.

From Eq. (25), for a specified incident wavelength, the slit width uniquely determines the truncation point α_t. From the theoretical analysis in Section III, the most relevant attribute of a particular Ronchi grating is its α_t truncation point with respect to the location of some particular j^{th} order. The three Ronchi gratings used in this investigation are uniquely characterized by the respective slit widths $w = 833\ nm$, $1000\ nm$, and $1250\ nm$. From Eqs. (25) and (40), $j(w) = 2w/\lambda$ gives a continuum of w-dependent truncation points relative to the j^{th} integer diffraction orders that is

$$j(w) = 2.63,\ 3.16,\ \text{and}\ 3.94 \tag{44}$$

for the three respective slit widths. In the present investigation, $\lambda = 633\ nm$ is invariant. Accordingly, the individual gratings are also uniquely characterized by the Eq. (44) continuum $j(w)$-equivalent truncation points. A Ronchi grating of some arbitrary slit width w is denoted as $G[j(w)]$ or simply G. Conversely, a grating identified with a numerical $j(w)$-equivalent truncation point identifies a particular grating with an implicitly expressed slit width. This use of $j(w)$ continues the convention in which variables are most instructively identified by the critical j-equivalent truncation value.

In this convention we are reminded that a grating such as $G(3)$ has truncations precisely bisecting the $\pm 3^{rd}$ orders whereas a grating $G(3-)$ has truncations marginally exclusive of the $\pm 3^{rd}$ orders i.e. truncations at the respective interior nulls of the $\pm 3^{rd}$ peaks. Extending this to the $j(w)$ continuum, a particular grating $G(2.63)$ has an implied slit width $w = 833\ nm$. The truncation point at $j = 2.63$ is exclusive of the $\pm 3^{rd}$ orders but only approximately satisfies the marginal exclusion of those orders specified by $j = 3-$. Similarly, a grating $G(3.16)$ implies $w = 1000\ nm$ and includes the $\pm 3^{rd}$ orders, but the truncation point at $j = 3.16$ is not marginal as it is for $j = 3+$. Despite the lack of truncations marginally close to $j = 3$ for $G(2.63)$ and for $G(3.16)$, these gratings are nevertheless predicted to yield orders that are respectively significantly enriched and depleted.

The final grating, $G(3.94)$ with $w = 1250\ nm$, is included to provide for a control experiment since the j-equivalent truncation point very closely matches the null orders at $j = 4$. See Fig. 7. Gratings with a j-equivalent truncation in the immediate neighborhood of $j = 4$ are predicted to provide orders that are ordinary. Consequently, $G(3.94)$ orders are expected to have no significant net energy transfer from coupling and should then exhibit no duality violation.

D. Calculation methods

Data are acquired with one of the three Ronchi gratings in the Fig. 10 position of G. Since the Gaussian beam diameters of the coupled Φ_G and Φ_R are not equal over the coupling path as a result of lenses $L1$ and $L2$, we necessarily undertake the examination of coupling phenomena with the extensive variables E and P rather than their respective intensive flux densities irradiance I and wave intensity $W = |\Phi|^2$. We continue the use of Φ_G and Φ_R as general identifiers of the respective beams, but we are reminded that these wave functions

in LRQM are exclusive of the energy quanta residing on those beams.

The basic premise of beam coupling is that a duality modulated beam equilibrates with an ordinary beam by a net transfer of energy quanta that leaves the wave structures of both beams unchanged and ideally converges the occupation values toward a common value. This convergence objective constitutes criterion (1). For this idealized coupling, a fully equilibrated state is achieved as Φ_G and Φ_R approach the end of the coupling path giving the equality

$$\Omega_{Gc} = \Omega_{Rc}. \tag{45}$$

We use the added subscript "c" on variables such as Ω to denote values at the end of the coupling path where equilibration of Φ_G and Φ_R has potentially altered those values relative to their respective values without Φ_G and Φ_R simultaneously present on the coupling path for those same variables.

Under a criterion (2), Φ_R should ideally serve as an infinite source for a depleted Φ_G or an infinite sink for an enriched Φ_G in the equilibration process. In the present case with

$$P_R \gg P_G$$

satisfied by a respective ratio of $\sim 100 : 1$ for these respective probabilities, we have an approximation of criterion (2) leaving the final equilibrated Φ_G and Φ_R both as ordinary and extending the Eq. (45) Ω equality to a unit-valued ordinary value,

$$\Omega_{Gc} = \Omega_{Rc} = 1. \tag{46}$$

If Φ_G is depleted or enriched as it emerges from a grating G, a net transfer of energy ΔE will occur between Φ_G and Φ_R that changes the initial grating-emergent energy E_G of Φ_G to

$$E_{Gc} = E_G \pm \Delta E \tag{47}$$

as the coupling path terminus is approached. A positive-signed ΔE corresponds to an energy gained by Φ_G in a transfer from Φ_R where Φ_G had initially been depleted. Similarly, if Φ_G had initially been enriched, ΔE is negatively signed. Alternatively, if Φ_G emerging from G is initially ordinary, no net transfer occurs and ΔE is zero.

The coupling equilibration of Φ_G to an ordinary state (if it is not already in an ordinary state) provides at the coupling path terminus in our arbitrary units the important result

$$P_G = E_{Gc}. \tag{48}$$

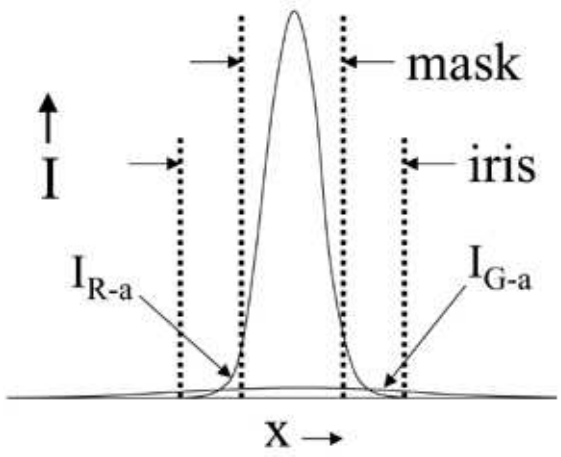

FIG. 12: Graphical depiction of irradiances at the coupling path terminus showing, in particular, the respective Φ_G and Φ_R annular beam irradiances I_{G-a} and I_{R-a} incident on the detector Det.

A sampling of this E_{Gc} is readily acquired by the detector.

Under idealized criterion (3), Φ_R is entirely excluded from the detector annular sampling region. In the present Fig. 11 configuration with the given beam parameters, the $\sim 100:1$ ratio of Φ_R probabilities P_{R-m} blocked by the B_m mask and P_{R-a} incident on the detector sampling region approximates criterion (3) as depicted in the Fig. 12 graph of irradiances.

The Fig. 13 oscilloscope pattern for the detector sampling with the chopper wheel in motion is a square wave of the pulsed Φ_G energy with a baseline biased by some steady state energy on Φ_R residually in the annular sampling field as well as any background level. Then the oscilloscope peak height measurement of the square wave

$$\begin{aligned} \Delta V_{Gc} &= \kappa E_{Gc} \\ &= \kappa P_G \end{aligned} \tag{49}$$

gives the beam's post-coupled energy and the Φ_G probability as well because of Eq. (48) to within a multiplicative constant κ. Chopper wheel pulsing of the Φ_G beam enables a peak height measurement of the square wave that automatically separates the detector sampling of E_{Gc} from any steady-state bias sources. For acquisition with a particular Ronchi grating G in position, the chopper wheel transmits and blocks Φ_G for equal 5 msec time intervals giving 10 msec cycles in generating a square wave pulse train transmitted to the oscilloscope from the detector amplifier.

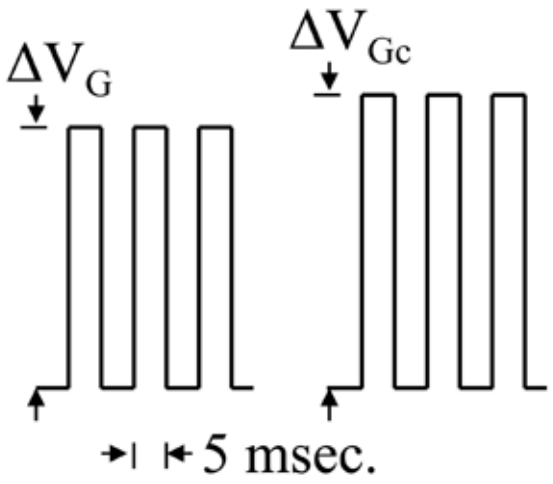

FIG. 13: Square-wave pulse outputs from detector amplifier (not to scale) for an initially depleted Φ_G. The measured pulse height ΔV_G with B_R blocking Φ_R increases to ΔV_{Gc} by equilibration transfer of irradiance from Φ_R on the coupling path.

After ΔV_{Gc} is acquired, Φ_R is blocked from the coupling path by B_R. The detector then samples the same annular region of Φ_G but now the peak height measurement

$$\Delta V_G = \kappa E_G \tag{50}$$

provides the beam's grating-emergent energy E_G, unmodified by coupling, to within the same multiplicative constant κ. The vital significance of these two detector measurements is that their ratio

$$\begin{aligned} \frac{\Delta V_G}{\Delta V_{Gc}} &= \frac{E_G}{P_G} \\ &= \Omega_{G\,ex} \end{aligned} \tag{51}$$

which is the experimentally determined occupation value from a single pair of measurements ΔV_{Gc} and ΔV_G. The subscript "ex" has been added to clearly identify this quantity as experimentally determined. The final averaged $\Omega_{G\,ex}$ reported in the next subsection for each of the three gratings studied are computed from multiple Eq. (51) determinations which are themselves averages of ~ 100 pulse cycles.

The theoretical counterpart to those final $\Omega_{G\,ex}$ experimental values is the Eq. (41)

function

$$\Omega_{r;0.5}(\alpha_t) = \Omega_{r;0.5}(\pi w/\lambda)$$
$$\equiv \Omega_{G[j(w)]\ th}, \tag{52}$$

shown in Fig. 7 and re-designated here as $\Omega_{G[j(w)]\ th}$ since the wavelength is invariant at $\lambda = 633\ nm$, G is uniquely characterized by the continuum value $j(w)$, and the added subscript "th" explicitly emphasizes the theoretical basis of the function.

In the foregoing method for calculating Ω from experimental measurements, it is necessary to cast the equations in terms of the directly detectable beam energies (as derived from beam powers) in order to infer the beam probabilities which are themselves not readily amenable to direct measurement. However, it is probability creation and annihilation that is of fundamental significance to duality violation in LRQM and therefore it is important from a theoretical perspective to explicitly express the resultant occupation value entirely in terms of probability.

For the general conditions of an ordinary output

$$\Omega_o = \frac{E_o}{P_o} = 1$$

and a resultant

$$\Omega_r = \frac{E_r}{P_r}.$$

With energy conservation

$$E_o = E_r$$

in the transition and identifying

$$P_r = P_o \pm \Delta P, \tag{53}$$

we have the equation

$$\Omega_r = \left(1 \pm \frac{\Delta P}{P_o}\right)^{-1} \tag{54}$$

where a positive sign represents ΔP probability creation and a negative sign represents ΔP probability annihilation.

E. Experimental results

Consistent with the notation in Eq. (52), the experimentally determined $\Omega_{G[j(w)]\ ex}$ values specific to the three gratings are $\Omega_{G(2.63)\ ex}$, $\Omega_{G(3.16)\ ex}$, and $\Omega_{G(3.94)\ ex}$.

The three experimental values $\Omega_{G\ ex}$ are plotted for comparison on the Fig. 7 theoretically predicted $\Omega_{G[j(w)]\ th}$. The experimental values $\Omega_{G(2.63)\ ex} = 1.015 \pm 0.003$ with a duality modulation of $+1.5\%$, $\Omega_{G(3.16)\ ex} = 0.982 \pm 0.003$ with a duality modulation of -1.8%, and $\Omega_{G(3.94)\ ex} = 0.998 \pm 0.003$ with a duality modulation of -0.2% are in good agreement with the theoretically predicted $\Omega_{G[j(w)]\ th}$ function for LRQM shown in Fig. 7. At the most fundamental level, quite independent from the LRQM theoretical basis presented here, any experimentally significant $\Omega_{G[j(w)]\ ex}$ deviations from unity demonstrate net transfers of energy during coupling that are inconsistent with PIQM.

F. Analysis of biased error

We conclude this section with an analysis of the three idealized coupling criteria identified in subsection D:

(1) The coupling path has perfect equilibration efficiency.

(2) Φ_R serves as an infinite source or sink.

(3) Φ_R is totally excluded from the detector sampling region by the mask on B_m.

As a practical matter these criteria are not fully achieved in the Figs. 10 and 11 apparatus and, accompanying the usual statistical dispersion of measured values, there are biased (non-random) sources of error present related to these criteria. We show below that these sources cause the experimentally measured $\Omega_{G\ ex}$ to underestimate the duality modulation, i.e. the actual magnitudes of the duality violations are larger than that of the current experimentally measured duality modulations. Moreover, we show that the magnitudes of the underestimates are not a significant fraction of their respective duality modulations. Despite the smallness of these underestimates, we include the biased error analysis here as an exercise in completeness and in the interests of identifying how the measurements can be optimized. These criteria and calculation of Ω underestimates are examined in greater detail in ref. [6].

Criterion (1) relates to an idealized coupling of two beams that fully equilibrates them to a common Ω. This equilibration is mediated by the physical proximity of the two beams and the longitudinal extent of that proximity. Both of these factors are addressed in the current experimental configuration by the coaxial propagation of these beams on a 2000 mm coupling path and the iris diameter.

Matching of the respective beam Gaussian diameters along the coupling path is necessarily altered by deliberate convergence of Φ_R onto the B_m mask in order to provide substantial separation of that beam from the detector annular sampling region. Nevertheless, this configuration still provides for effective coupling over the 2000 mm path. Longer coupling paths have been examined in the interests of potentially improving the coupling efficiency, but with no significant change in $\Omega_{G\ ex}$ observed, the 2000 mm path was retained.

Similarly, for the Fig. 11 beam configuration, coupling path efficiency is further optimized by maximizing radial equilibration between Φ_G and Φ_R. This is achieved by confining the sampled Φ_G to an annular region most closely coupled to the convergent Φ_R using a minimal iris setting (that still admits sufficient Φ_G beam power for measurement).

In any case, an incomplete equilibration arising from a non-ideal coupling implies that the ΔE transfer is less than it would be if $\Omega_{Gc} \to 1$. As a result, the apparent P_G equated to the measured E_{Gc} would be underestimated for depletion and overestimated for enrichment yielding an underestimated magnitude of duality modulation for both.

In order to demonstrate the magnitude of the duality modulation underestimate for the not fully achieved criteria (2) and (3), it is most useful to begin with idealized experimental values $\Omega_{G(3-)\ ex,id} = 1.025$ and $\Omega_{G(3+)\ ex,id} = 0.975$ for which criteria (2) and (3) are achieved in principle and calculate the respective apparent values $\Omega_{G(3\pm)\ ex,ap}$.

For criterion (2), if Φ_R has only a finite probability P_R, perfect coupling path equilibration from criterion (1) does still provide equalized final occupation values

$$\Omega_{G(3\pm)c\ ex} = \Omega_{Rc\ ex,id} \neq 1 \tag{55}$$

but because of the finite P_R, the initial $\Omega_{G(3\pm)\ ex,id}$ and Ω_R are mutually convergent on a non-unit value. For the intensive Ω's and extensive P's and E's, it can readily be shown that

$$\begin{aligned} \Omega_{G(3\pm)c\ ex} &= \frac{E_G + E_R}{P_G + P_R} \\ &= \Omega_{G\ ex,id}\frac{P_G}{P_G + P_R} + \Omega_R\frac{P_R}{P_G + P_R} \end{aligned} \tag{56}$$

where, for the initially ordinary Φ_R, $E_R = P_R$ and $\Omega_R = 1$.[6]

To examine this expression in the context of the present experiment, where $E_R \approx 100E_G$, we note that the probabilities are also approximately related by $P_R \approx 100P_G$ despite a small inequality of E_G and P_G for a small duality modulation of the initial Φ_G. These energies,

which are measurable by detector, may be substituted for the respective probabilities in the coefficients $P_G/(P_G + P_R)$ and $P_R/(P_G + P_R)$. This substitution introduces only a second order error in Eq. (56) since the respective $P \approx E$. Then

$$\Omega_{G(3\pm)c\ ex} = \frac{1}{101}\Omega_{G(3\pm)\ ex,id} + \frac{100}{101}. \tag{57}$$

For $\Omega_{G(3-)\ ex,id} = 1.025$,

$$\begin{aligned}\Omega_{G(3-)c\ ex} &= 1.0002 \\ &= \Omega_{G(3-)c\ ex,id} \\ &= \frac{E_{Gc}}{P_G} \\ &= \Omega_{Rc\ ex}.\end{aligned} \tag{58}$$

Then, for the finite Φ_R that does not yield a fully realized criterion (2), $E_{Gc} = 1.0002P_G$ is treated as P_G and the apparent experimentally measured occupation value

$$\Omega_{G(3-)\ ex,ap} = \frac{E_G}{E_{Gc}} = \frac{E_G}{1.0002P_G} = \frac{1}{1.0002}\Omega_{G(3-)\ ex,id}. \tag{59}$$

From this result we find that the apparent $\Omega_{G(3-)\ ex,ap}$ is insignificantly smaller than the idealized $\Omega_{G(3-)\ ex,id}$ and the apparent duality modulation $\Omega_{G(3-)\ ex,ap} - 1$ is also insignificantly smaller than the idealized value.

Similarly, for $\Omega_{G(3+)\ ex,id}$ the apparent $\Omega_{G(3+)\ ex,ap}$ is insignificantly larger than the idealized $\Omega_{G(3+)\ ex,id}$ and the magnitude of the apparent duality modulation $\left|\Omega_{G(3+)\ ex,ap} - 1\right|$ is also insignificantly smaller than the idealized value.

Lastly, we consider deviation from criterion (3). In practice, the Gaussian tail of the convergent Φ_R beam spot always has some small but finite fraction of P_R outside the B_m mask into the annular sampling region. As a consequence, Φ_R is not completely separated from the annularly sampled Φ_G. Conversely, that sampling accepts a substantial fraction of P_G. The general significance of this incomplete separation relates again to an apparent discrepancy in ΔE transferred to or from Φ_G to produce an E_{Gc} that is presumed to have equivalence to P_G. In the equilibration process an equal ΔE is transferred respectively from or to Φ_R. Upon coupling, some large fraction F_G of ΔE transfers to or from Φ_G in the annular region while concurrently some small but finite fraction F_R of ΔE transfers respectively from or to Φ_R in the same annular region resulting in a diminished net energy transfer in the annular measurement region.

This dependency of the occupation value on the portion of Φ_R in the annular sampling region is given by an apparent

$$\Omega_{G(3\pm)\ ex,ap} = \frac{F_G E_G}{F_G E_G \pm (F_G \Delta E - F_R \Delta E)} \tag{60}$$

where $\pm$ applies respectively to an initially depleted or enriched Φ_G.[6] To put this error into perspective with regard to the apparatus of the present experiment, $F_G \approx 0.4$ and $F_R \approx 0.01$. For the idealized $\Omega_{G(3\pm)\ ex,id}$, the magnitude of the duality modulation is $\left|\Omega_{G(3\pm)\ ex,id} - 1\right| = \Delta E/E_G = 0.025$. With these values, an idealized 2.5% magnitude of duality modulation for both depleted and enriched Φ_G is again underestimated as an apparent insignificantly smaller magnitude.

We conclude that the close approximations to the criteria (1), (2), and (3) for the beam parameters in the present experiment provide apparent $\Omega_{G\ ex,ap}$ values that differ insignificantly from idealized $\Omega_{G\ ex,id}$ values. Consequently, no compensating adjustment of experimental results $\Omega_{G\ ex}$ in the previous subsection is required with regard to the coupling criteria.

V. DISCUSSION

A viable locally real alternative to the probabilistic interpretation of quantum mechanics PIQM must necessarily be in agreement with performed experiments and must provide a self-consistent theoretical basis for representing quantum mechanical phenomena.

We hypothesize that a comprehensive locally real representation of an underlying quantum mechanical formulation, LRQM, can be systematically constructed by providing for separable locally real wave-like and particle-like physical entities where the wave-like entity is represented on a covariant field of elementary oscillators generally in ground state with relative non-coherence.[4] A photon in this representation consists of a wave packet of these ground state oscillators in relative coherence, i.e. the wave-like entity. The particle-like entity, i.e. the energy quantum, consists of a raised energy state of one of these oscillators in coherent motion. The density of these oscillators in relative coherence at a particular location on the wave packet Φ is given by $|\Phi|^2$. This density of oscillators in relative coherent motion represents a small fraction of the total density of field oscillators at any given point. Consistent with Born's rule, $|\Phi|^2$ provides the probability flux density for the location of the energy quantum on the wave packet. For ordinary ($\Omega = 1$) photons, the integration of

$|\Phi|^2$ over all space (essentially, over the entire wave packet) yields a value that is in strict proportion to the unit energy quantum consistent with the PIQM principle of duality.

We emphasize that these LRQM interpretations, restricted to a simple system such as an ordinary discrete photon, are not measurably distinguishable from those of PIQM. Differentiability arises when the structure of the wave packet is altered in such a way that local probability on a photon is not conserved. For correlated entities, this is shown in ref. [4] to be a constraint on the ensemble of quantum states in Hilbert space that results in a probability loss on one of the correlated entities. The locally real solution, which is independent of Bell's Theorem [5], is consistent with the underlying quantum mechanical formalism and agrees with performed experiments.

In the present investigation of duality, non-conservation of probability is again the factor distinguishing LRQM from PIQM. With respect to duality, the probability non-conservation is manifested as an alteration of the local flux density $|\Phi|^2$ of oscillators in relative coherence. At the simplest level, the wave packet of an ordinary discrete photon traversing a beam splitter emerges as a pair of spatially similar wave packets along the transmissive and reflective output channels but with relative oscillator coherence densities reduced to $T\,|\Phi|^2$ and $R\,|\Phi|^2$, respectively where T is the transmission factor and R is the reflection factor of the beam splitter. The energy quantum transfers onto one of these two packets, again consistent with Born's rule. Probability is conserved when summed over both output channels ($T + R = 1$) and PIQM retains duality by invoking a non-local probabilistic (non-real) interpretation of this phenomenon. From the perspective of LRQM, the two emergent packets, only one of which is occupied by the energy quantum, both exhibit physical distinctions from the incident photon. However, the testability of these distinctions at the discrete level is problematic. This difficulty is circumvented here by going to the continuous wave (cw) regime and using a grating system presumptively generating duality-modulated beams since even very modest duality modulations are definitively testable in the cw regime.

The LRQM treatment of probability as a relative quantity can be demonstrated from the perspective of the densities of the field oscillators in coherent motion on the resultant diffraction beams emergent from a grating near threshold. For example, $\sim 2.5\%$ of the output probability that forms the resultant probability is annihilated in the near zone of grating $G(3-)$. Equivalently, this translates to a $\sim 2.5\%$ reduction in the coherent oscillator density on each of the $G(3-)$ resultant orders. However, as the output energy quanta in

the near zone of $G(3-)$ transfer onto the resultants, the proportionate $\sim 2.5\%$ reduction in the coherent oscillator density on each does not alter the relative distribution of the total quanta onto those orders. Indeed, any proportionate reduction or increase in coherent oscillator density on a complete set of resultant channels does not change the distribution of a given set of quanta transferring onto those channels. Probability, treated as a measure of the physical coherent oscillator density, is appreciated as a relative quantity expressing the expectation of quanta transferring to a particular channel.[9]

Conversely, the motivation to compactly fold conservation of the particle-like energy quantum in with the distributional probability results in a PIQM profoundly distinctive from LRQM. The PIQM normalization of the integrated $|\Phi|^2$ over all space effectively elevates the wave-like probability to equivalence with the particle-like energy quantum. This is really the fundamental statement of duality. An objective review of the distinctions imposed by PIQM duality is given by Rabinowitz.[20]

In PIQM energy quanta and probability are then dual manifestations of a single entity, the "photon". However, when superposition states such as those created by a beam splitter are considered, PIQM is forced to impose the properties of non-locality and non-reality which particularly distinguish that interpretation from LRQM.

Alternatively, in the comprehensive LRQM that emerges, the field coherence states are represented by the wave functions that exhibit probability non-conservation for particular quantum phenomena. These wave functions, freed from the constraint of duality-imposed renormalization, "complete" the underlying quantum mechanical formalism in the regard that the quantum phenomena are then representable as locally real. In this context, Einstein, Podolsky, and Rosen had referred to objective properties of a physical system that are represented by parameters which they called "elements of reality".[2] In common usage these elements have since, unfortunately, been re-identified as "hidden variables". Ferrero, Marshall, and Santos present a compelling argument for the inappropriateness of this re-identification. Their argument has application here since the LRQM wave function is shown to express objective properties before any measurement is made on it as they prescribe in ref. [21]. Moreover, the objective properties of that wave function can realized by physical measurement. The intensity $|\Phi|^2$ of a beam is disproportionate to that beam's irradiance for a non-ordinary beam. That disproportion is measurable from the energy quanta transfer that occurs during equilibration coupling of that beam with an ordinary beam.

From the perspective of PIQM, for which probability is systematically conserved in the preparation of the normalized wave function, the variables that would provide locality appear to be hidden since phenomena that distinguish PIQM from LRQM are associated with non-conservation of probability.

Ferrero, Marshall, and Santos postulate that "in spite of the spectacular success of quantum mechanics, it is worthwhile exploring (small) modifications of the formalism in order to ensure compatibility with local realism." [21] This comment was made in the support of seeking a locally real theory that naturally obviates entanglement, but necessarily implies extension to an encompassing theory that also naturally excludes quantum phenomena that invoke non-locality such as duality. The objective posed by Ferrero, Marshall, and Santos is intrinsic to LRQM by incorporating the underlying quantum formalism modified only by the omission of probability renormalization in transitional processes. The resultant LRQM is broadly consistent with PIQM predictions and performed experiments while providing for a local reality-based representation.

VI. CONCLUSIONS

The experiment reported here provides a highly reproducible violation of quantum mechanical duality using an apparatus configured with two independent HeNe lasers and readily available components. The determination of that duality violation resolves to easily measured variations in continuous wave laser beam power, variations predicted by a locally real representation of quantum mechanics but excluded by the probabilistic interpretation of quantum mechanics.

---

[1] V. L. Lepore and F. Selleri, Found. Phys. Lett. **3**, 203 (1990).

[2] A. Einstein, B. Podolsky, and N. Rosen, Phys. Rev. **47**, 777 (1935).

[3] K. R. Popper, in *Quantum Theory and the Schism in Physics*, (Rowman and Littlefield, Totowa, NJ,1982).

[4] S. Mirell, Phys. Rev. A **65**, 032102 (2002).

[5] J. S. Bell, Physics (N.Y.) **1,** 195 (1964).

[6] D. Mirell and S. Mirell, e-print quant-ph/0509028.

[7] L. de Broglie, in *Electrons et Photons*, (Gauthier-Villars, Paris,1928); *The Current Interpretation of Wave Mechanics: A Critical Study* (Elsevier, Amsterdam, 1969).

[8] M. Born, Zeitschrift für Physik **37**, 863 (1926).

[9] D. S. Saxon, in *Elementary Quantum Mechanics*, (Holden-Day, Inc., San Francisco, 1964).

[10] J. R. Croca, A. Garuccio, V. L. Lepore, and R. N. Moreira, Found. Phys. Lett. **3**, 557 (1990); L. J. Wang, X. Y. Zou, and L. Mandel, Phys. Rev. Lett. **66**, 1111 (1991); J. R. Croca, A. Garuccio, V. L. Lepore, and R. N. Moreira, Phys. Rev. Lett. **68**, 3813 (1992); X. Y. Zou, T. P. Grayson, L. J. Wang, and L. Mandel, Phys. Rev. Lett. **68**, 3814 (1992).

[11] F. Selleri, Phys. Lett. A **120**, 371 (1987); M. Lai and J. -C. Diels, J. Opt. Soc. Am. B **9**, 2290 (1992); L. Hardy, Phys. Lett. A **167**, 11 (1992); R. B. Griffiths, Phys. Lett. A **178**, 17 (1993); R. Folman and Z. Vager, Found. Phys. Lett. **8**, 55 (1995); W. De Baere, Found. Phys. Lett. **10**, 119 (1997); C. Braig, P. Zarda, C. Kurtsiefer, and H. Weinfurter, Appl. Phys. B: Lasers and Optics **76**, 113 (2003).

[12] J. C. Maxwell, in *Theory of Heat*, (Longmans, Green, and Co., London, 1871).

[13] W. C. Elmore and M. A. Heald, in *Physics of Waves*, (McGraw-Hill Book Company, New York, 1969).

[14] R. W. Wood, Philos. Mag. **4**, 396 (1902).

[15] J. W. S. Rayleigh, Philos. Mag. **14**, 60 (1907).

[16] G. F. Hull, Am. J. Phys. **17**, 559 (1949); A. T. Forrester, R. A. Gudmundsen, and P. O. Johnson, Phys. Rev. **99**, 1691 (1955); A. Javan, E. A. Ballik, and W. L. Bond, J. Opt. Soc. Am. **52**, 96 (1962); D. R. Herriott, J. Opt. Soc. Am. **52**, 31 (1962); B. J. McMurty and A. E. Siegman, Appl. Opt. **1**, 51 (1962); M. L. Lipsett and L. Mandel, Nature **199**, 553 (1963); G. Magyar and L. Mandel, Nature **198**, 255 (1963); R. L. Pfleegor and L. Mandel, Phys. Rev. **159**, 1084 (1967).

[17] H. Paul, Rev. Mod. Phys. **58**, 209 (1986).

[18] P. A. M. Dirac, in *The Principles of Quantum Mechanics*, (Oxford University Press, Oxford, 1930).

[19] L. Mandel, Phys. Rev. **134** A10 (1964).

[20] M. Rabinowitz, Mod. Phys. Lett. B **9**, 783 (1995).

[21] M. Ferrero, T. W. Marshall, and E. Santos, Am. J. Phys. **58**, 683 (1990).